



A glimmer of the eastern Adriatic: Compositional analysis of first-millennium BCE glass from Histria (Istria, Croatia)

Ana Franjić ^{a,*}, Ian C. Freestone ^b, Gry Barfod ^c, Ulrike Sommer ^b, Patrick Degryse ^a

^a Division of Geology, Department of Earth and Environmental Sciences, KU Leuven, Celestijnenlaan 200E – Bus 2411, 3001 Leuven, Belgium

^b UCL Institute of Archaeology, 31– 34 Gordon Square, London WC1H 0PY, United Kingdom

^c Cobb Meadow Research, Camden, ME, USA

ARTICLE INFO

Keywords:

Histria
Iron Age
Glass beads
EPMA
LA-ICP-MS
Long-distance trade

ABSTRACT

Finds of glass artefacts from prehistoric Histria (present-day Istria, Croatia) are rare. This study presents compositions of thirty-eight glass beads and vessels spanning from the Late Bronze to the Late Iron Age analysed by EPMA, with a selected subset analysed using LA-ICP-MS. Levantine natron glass with Al_2O_3 around 2.5% is the most abundant compositional group. However, several other natron glass types have been detected from the early first millennium CE, including black natron glass with high Li, Th and U, corresponding to black glass type found elsewhere in Europe and the Middle East. Blue beads coloured with cobalt alum are decorated with lead antimonate yellow glass containing alumina concentrations below 1%, and, in spite of the very marked changes in elemental composition resulting from the colourant additions, these two glasses show similarities in elements such as K, Ca, Sr, Ba, and Zr which may reflect production in the same workshop. Two samples, dated to the transition from the Late Bronze to the Early Iron Age, are of the low-magnesia-high-potash (LMHK) type from the Veneto, and two further, slightly later samples are plant ash-based glasses from Mesopotamia. Overall, the range in glass types demonstrates strong links between Histria and Italic prehistoric communities, and Histrian participation in established long-distance trade networks from a very early period.

1. Introduction

Between research into the beginnings of glassmaking in the Bronze Age and the minutiae of the elaborate and large-scale Roman glass production, lies Iron Age glass, with its mechanisms of production and trade still somewhat shrouded in mystery. Recent decades, however, have seen many interesting case-studies on the subject, which are slowly beginning to unravel the conditions of glass production, trade, and use during the first millennium BCE (among others, see Arletti et al. 2012; Conte et al. 2016, 2018; Oikonomou 2018; Reade and Privat 2016; Rolland 2021).

Among the growing amount of data on Iron Age glass from northern and central Europe, Greece, and the Mediterranean, there is a lacuna in the data from South East Europe. The present study is a first step towards filling this lacuna, by defining the chemical composition of glass encountered in the region, and by tracing the social connections and influences glass might have generated. The departure point of this inquiry is set in the eastern Adriatic, more precisely its northern reaches. Situated below the head of the Adriatic, *Histria*, or present-day Istria, is

the largest peninsula in the Adriatic Sea. It overlooks the last—or first—stop on the long-distance sea routes extending from the Mediterranean to North Europe. This distinct geostrategic position of the Istrian peninsula influenced the protohistoric developments in this region, facilitating connections with neighbouring as well as distant societies.

During the first millennium BCE, most of the Istrian peninsula was inhabited by communities referred to as *Histri*. They are mentioned by a number of ancient authors (Hecataeus, Pseudo-Scylax, Pseudo-Scymnus, Strabo, Livy, Appian, Ptolemy), and are described as Illyrians, related to the neighbouring Liburni to the east, and the Veneti to the west (Mihovilić 2013a: 24–6). They are also depicted as “notorious pirates”, who attacked Roman supply ships (Stipčević 1974: 46; Wilkes 1992: 185; Livy 1996: 10.2, 21.16). Histrian territory was bordered by the Učka mountain in the northeast, the Rijana river in the west, and the Raša river to the east (Fig. 1). After much struggle, Histria succumbed to the Romans in the late third to early second century BCE, and eventually, in the course of Augustus’ administrative subdivision of Italy, became part of *Regio X Venetia et Histria* (Wilkes 1992: 186, 209).

The geomorphology of the peninsula and the indented coastline

* Corresponding author.

E-mail address: ana.franjic@kuleuven.be (A. Franjić).

favoured the formation of settlements on elevated ground, above rivers and channels, providing good surveillance over the sea routes. From the end of the Early Bronze Age, Histria was a part of the Castellieri Culture, extending through present-day Friuli Venezia Giulia, Istria, and Dalmatia, and recognisable by its systems of hillforts, of which more than three hundred have been attested in Istria at present (Ćučković 2017; Mihovilić 2013a: 36; Mihovilić 2013b: 1; Gabrovec and Mihovilić 1987: 298; Tomas 2016: 77). Some of the sites remained in use throughout the first millennium BCE.

The material culture of the Histri is characterised by strong influences from Veneto, Etruria, Este, Picenum, Apulia, and Greek Attica (Gabrovec and Mihovilić 1987: 293; Majnarić-Pandžić 1998: 254; Mihovilić 2007: 619). Many luxury and imported items from these regions—feasting sets, situlae, machairai swords, Baltic amber, Etruscan fans, Greek and Daunian pottery, among others—attest to their relationship with the wider region and are presumed to have been integral for the construction of (elite) Histrian identity, with Etruscan influence particularly evident (Stoddart 2014: 266, 277). Alongside luxury imports, in the seventh and sixth century BCE Histri even produced their own monumental stone sculptures, influenced by the Greek archaic style (Stoddart 2014: 278; Mihovilić 2013a: 330). Furthermore, Histria is the only area on the eastern Adriatic where a Mycenaean presence is (inconclusively) suggested, due to various finds (fine pottery, tripods, animal bones) that can be related to Mycenae (Gavranović 2016: 125; Tomas 2016: 77–8). This would suggest very early contacts between Histria and other Mediterranean cultures.

Archaeological excavations in the region have mostly been conducted at hillfort cemeteries (Mihovilić 2013a: 32; cf. Amoroso 1885, 1889; Baćić 1958; Benussi 1927; Betic 2005; Cestnik 2009; Gnirs 1925; Hoernes 1894; Marchesetti 1884; Matijašić 1982–3; Mihovilić 1972, 1979; Mladin 1969; Moretti 1983; Orlić 2011; Petešić 2011; Sakara Sučević 2004; Starac 2006, 2007, 2008, 2011; Urem 2012, among others). However, glass artefacts were not given particular attention. Overall, it can be presumed that the amount of glass in burials is likely underrepresented, as cremation was the main burial rite, and stray finds of jewellery were often recovered from the *ustrinum*, a separate location for the cremation of the deceased and the performance of funeral ceremonies adjacent to the cemetery (Gabrovec and Mihovilić 1987: 321–22; Urem 2012: 16–17).

2. Materials

Sampling took place at the Archaeological Museum of Istria, using materials recovered from six cemeteries associated with Histrian

hillforts (Figs. 1–2, Table 1). Some of these hillforts were inhabited for a very long period—from the twelfth century BCE onwards (Lim, Nesactium, Picugi)—and the cemeteries are often organised into clan groups (Urem 2012: 9). Some of the sites have been better researched than others: for example, the Lim hillfort, situated above the Lim channel, is one of the few systematically excavated Histrian sites, and has also helped define the absolute chronology of the Iron Age in Istria (Komšo 2012: 7; Mihovilić 1972).

Glass is found as grave goods, often alongside prestigious imports (Mihovilić 2013a: 96; Zaninović 2007: 122), and is mostly dated indirectly, through other, more diagnostic items. Some samples have been retrieved from closed grave units: Mariškići, a dual, adult and child cremation grave dated to the third to second century BCE, from a hillfort cemetery located below the ruins of a medieval castle of Stari Lupoglav (Mihovilić and Rajić Šikanjic 2016: 57–59); St. Martin, featuring urn burials from the habitation area of St Martin hillfort, but without a secure date (Janković et al. 2015: 945); Lim hillfort, with urn burials from the cemetery (Urem 2012: 9–10). Samples from Nesactium—the largest Histrian hillfort, surrounded by ten further subsidiary hillforts, and considered to have been the capital of Histri (Mihovilić 2013a: 330)—were retrieved from the *ustrinum*, located below a Roman temple built over the site (Gestnik 2009: 81). Samples from Pula, the Picugi triple hillfort, Nesactium, and Kaštelir are poorly documented and their exact location within the cemetery context is not recorded.

The analysed Histrian beads comprise of several bead types, colours and decorations (Figs. 2–3). Following the typologies of Brugmann (2004), Haevernick (1978), Spaer (2001), Venclová (1990), and Haevernick and Dobiat (1987), the most frequent types are globular beads (55 % of the studied assemblage), followed by annular beads (13 %). The assemblage contains several distinct types, such as the head bead (Pu 13), barrel-shaped beads (Pu 3, 7) amphora-shaped pendant (Pu 20), and grain-of-wheat bead (Pu 40). The vessel examples are fragmented, comprising rims and a handle (Pu 11, 14, 15). Most of the assemblage is either blue ($n = 16$) or colourless ($n = 21$), with the colourless beads being mostly undecorated, while the blue beads are mostly decorated with simple decoration, such as lines, ring eyes, and compound eyes.

3. Methods

Overall, 41 analyses of 38 glass items—35 beads and 3 vessel fragments—dated to the first millennium BCE (end of the Late Bronze Age–Late Iron Age, according to the region's periodisation) were conducted (Table 1, Fig. 2). Samples, usually around 1 mm in width, were taken using a carbide-tip scribe. Two samples of different coloured

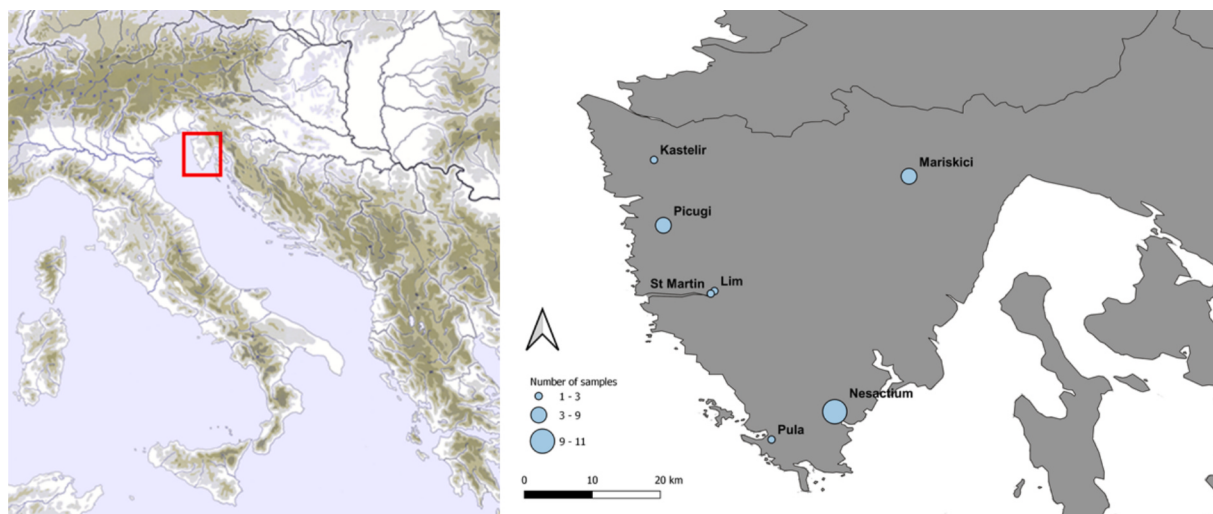


Fig. 1. The Istrian peninsula, with sites from which the material from this study has been retrieved.



Fig. 2. Beads and vessel fragments analysed for this study.

glasses were obtained from some multi-coloured artefacts (these have an additional letter in the sample name indicating the sample's colour). The samples were ground flat and mounted in resin blocks, and then ground, polished, and carbon-coated. A JEOL JXA-8100 Electron Probe Micro-analyser with three wavelength dispersive spectrometers (EPMA-WDS) was used for the measurement of major and minor elements, and the analysis was carried out in the Wolfson Archaeological Science Laboratories at the UCL Institute of Archaeology.

Three area measurements for each sample were taken at the magnification of 800x, a working distance of 11 mm, an accelerating voltage of 20 kV, and a beam current of 50nA. Count time on each element peak was 30 s, and count time per background measurement was 10 s. Nineteen elements were analysed for each sample. The data was not normalised; the totals range from 95.6–100.76 %. Limits of detection were determined at 0.03 % based on measurements of Corning Museum Archaeological Glass Standards A and B (Adlington 2017; Brill 1999)—which were also used to assess precision and accuracy, estimated to be mostly better than 5 % for major and 10 % for minor elements, except for P₂O₅, TiO₂, ZnO and PbO in Corning A, and SnO₂ and PbO in Corning B (Supplementary Table 1).

Fifteen samples, chosen to represent the identified base glass types, were analysed for trace elements by Laser Ablation Inductively Coupled Plasma Mass Spectrometry (LA-ICP-MS) at the Aarhus Geochemistry and Isotope Research (AGiR) Platform laboratories of the Department of Geoscience, Aarhus University, Denmark. The analysis was conducted using an Agilent Technologies 7900 quadrupole ICP-MS coupled to a Resonetics 193-nm laser, with helium as the carrier gas. The laser parameters were set at 80.2 mJ, a 10 Hz pulse frequency, and a 60-μm spot size. Ablation time was 65 s: 30 s pre-ablation background analysis and 35 s of data collection time.

Standards were analysed at the beginning and end of the analytical session, and periodically after every eight analyses to correct for drift. The data are reported as a mean of three analyses of different areas of each specimen. The results were processed in Microsoft Excel using USGS synthetic reference glass standard GSE-1G as the internal calibration standard to correct for instrumental drift and matrix effects. The

Si-based normalization was applied to unknown samples; the Si counts in samples were matched to the SiO₂ concentrations independently measured by EPMA. Three external standards were used to monitor the quality of measurement: Atho-G, GSD-1G (Jochum et al. 2005; Guillong et al. 2005), and Corning B (Brill 1999). Accuracy and precision for all measured elements according to the standards was found to be mostly below 20 %, and below 2 %, respectively, based on 29 analysis over three days (Supplementary Table 2). Four-nine elements were quantified (Table 3).

4. Results

EPMA results are presented in Table 2 and trace elements in Table 3. Multivariate Analysis of the major elements identified three main compositional groups, one of which has four further subgroups (Fig. 4). The groups and subgroups can also be differentiated on the basis of their MgO and Al₂O₃ contents (Fig. 7). The majority of samples ($n = 37$) are soda-lime-silica glasses with low MgO and correspond to natron glass, two samples are soda plant ash glass and two are mixed alkali.

4.1. Group 1: Natron glass

Natron glass group can be subdivided into several subgroups based on the compositional differences which, in most cases, reflect the silica source(s).

Na1 ($n = 28$) comprises the majority of the beads and all of the vessels in the dataset. Major components correspond to typical natron glass from the eastern Mediterranean from the late first millennium BCE to the late first millennium CE ($\bar{x} = \text{SiO}_2 68.2\%; \text{CaO } 7.79\%; \text{Na}_2\text{O } 15.9\%; \text{Al}_2\text{O}_3 2.35\%; \text{TiO}_2 0.05\%; \text{Fe}_2\text{O}_3 0.53\%$). Several samples have elevated K₂O contents outside the normal natron range (Fig. 5). However, there is a correlation between K₂O and P₂O₅ suggesting that these glasses have been contaminated by fuel ash vapour in the manufacturing process, possibly due to prolonged melting (Barfod et al. 2022a,b; Paynter 2008; Rehren et al. 2010). Of the three samples showing the highest K₂O and P₂O₅ contents, Pu6t is depleted in chlorine, while Pu27

Table 1

List of analysed samples.

Sample	Site	Context	Date	Type	Shape	Colour	Decoration	Accession nr.
Pu1	Nesactium	Roman "Temple B" soil	700–100 BCE	fragment	n/a	colourless	n/a	p-40973
Pu2	Kastelir	unknown	800–100 BCE	bead	biconical	colourless	yellow lines and bosses	p-2156
Pu3	Lim hillfort	grave 60	1100–1000 BCE	bead	tubular	blue	horizontal lines; unpreserved	p-18994
Pu4	Nesactium	Roman "Temple B" soil	800–100 BCE	bead	globular	colourless	n/a	p-40972
Pu5	Nesactium	middle temple grave	800–100 BCE	bead	globular	blue	white and blue compound eyes	p-25252
Pu6	Lim hillfort	unit 759	800–100 BCE	bead	globular	colourless	n/a	p-18629
Pu7	Lim hillfort	grave 57	1100–1000 BCE	bead	tubular	blue	spirals; unpreserved	p-18956
Pu8	Nesactium	foundations of Roman temples B and C	1000–600 BCE	bead	annular	blue	eye; unpreserved	p-25269
Pu9	Nesactium	Roman temple C soil	200–100 BCE	glass	fragment	colourless	n/a	p-31725
Pu10	Pula	cemetery	1000–100 BCE	bead	globular	blue	yellow wave	10,536
Pu11	Nesactium	foundations of Roman temples B and C	1000–100 BCE	vessel	fragments	colourless	n/a	31,726
Pu12	Nesactium	foundations of Roman temples B and C	200–10 BCE	bead	globular	colourless	n/a	p-25273
Pu13	Nesactium	foundations of Roman temples B and C	700–100 BCE	bead	head-bead	blue	white and blue	31,723
Pu14	Nesactium	foundations of Roman temples B and C	1000–100 BCE	vessel	fragment	colourless	n/a	31,724
Pu15	Nesactium	foundations of Roman temples B and C	1000–100 BCE	vessel	handle	colourless	n/a	p-40759
Pu17	Pula	cemetery	1000–500 BCE	bead	globular	blue	blue	43,814
Pu18	Pula	cemetery	1000–500 BCE	bead	cylindrical	brown	n/a	9572
Pu19	Nesactium	beneath Early Christian Basilica altar	300–100 BCE	bead	globular	colourless	n/a	p-40141
Pu20	St.Martin	*grave	1000–100 BCE	pendant	amphora-shaped	colourless	n/a	40,583
Pu21	St.Martin	*grave	1000–100 BCE	bead	globular	colourless	n/a	40,578
Pu22	Mariškići	¥ dual cremation burial	300–100 BCE	bead	globular	colourless	n/a	p-42371
Pu23	Mariškići	¥ dual cremation burial	300–100 BCE	bead	annular	blue	n/a	p-42365-1
Pu24	Mariškići	¥ dual cremation burial	300–100 BCE	bead	globular	colourless	colourless bosses	p-42370
Pu25	Mariškići	¥ dual cremation burial	300–100 BCE	bead	globular	blue	yellow spiral	42,367
Pu26	Mariškići	¥ dual cremation burial	300–100 BCE	bead	globular	colourless	n/a	42,369
Pu27	Mariškići	¥ dual cremation burial	300–100 BCE	bead	annular	blue	unpreserved	p-42364
Pu28	Mariškići	¥ dual cremation burial	300–100 BCE	bead	cylindrical	blue	horizontal lines; unpreserved	42,366
Pu29	Picugi	cemetery	1000–500 BCE	bead	globular	colourless	n/a	p-44082
Pu30	Mariškići	*dual cremation burial	300–100 BCE	bead	globular	colourless	n/a	42,368
Pu31	Picugi	cemetery	1000–100 BCE	bead	globular	blue	yellow eyes and dots	p-44084
Pu32	Picugi	cemetery	1000–600 BCE	bead	wide annular	blue	yellow ring eyes	p-44083
Pu33	Picugi	cemetery	1000–100 BCE	bead	globular	colourless	n/a	p-44081
Pu34	Picugi	cemetery	1000–500 BCE	bead	globular	colourless	n/a	p-1557
Pu36	Mariškići	¥ dual cremation burial	300–100 BCE	bead	globular	blue	unpreserved	p-42365-2
Pu37	Picugi	cemetery	1000–600 BCE	bead	globular	blue	yellow ring eyes	p-1552
Pu38	Picugi	cemetery	600–100 BCE	bead	wide annular	colourless bluish	mid-section bosses	p-44080
Pu39	Picugi	cemetery	1000–600 BCE	bead	globular	blue	yellow ring eyes	p-1552
Pu40	Picugi	cemetery	600–100 BCE	bead	grain of wheat	amber	n/a	p-1557

and Pu28 have low chlorine and soda, consistent with long melting periods (cf. Barfod et al. 2022a, b). We note that such contamination can also arise when the object's surface comes in contact with the vapours from the fuel and when buried in the annealing ashes (Davis and Freestone 2018: 117). Furthermore, a similar trend can occur during cremation, as well as during the manufacture of the bead, as was noticed during the experimental reproduction of glass bracelets (Rolland 2015: 123, 2021: 41–43). However, in these instances elevated potash is a surface effect which diminishes with depth; given that our analysis was performed on cross sections and well beyond the surface and the suspected contamination zone, the observed elevated levels are more likely the result of prolonged melting.

Silica source-related trace elements of subgroup Na1, when normalised to the weathered continental crust (MUQ of Kamber et al. 2005), have positive Zr and Ba inflections and a relatively flat REE signal with a positive Eu anomaly (Fig. 6). Sr values in excess of 400 ppm (Table 3) are consistent with the use of coastal sand containing Holocene shell fragments (Freestone et al. 2003; Brems et al. 2013).

Na2 ($n = 2$). Two yellow glasses (Pu 32, Pu 39) have low MgO and K₂O concentrations ($\bar{x} = 0.27\%$, and 0.12% , respectively), and Na₂O concentration appears low as well ($\bar{x} = 10.3\%$). High Sb₂O₅ (3.67–3.77 %) and very high PbO (31.7–32.6 %), indicate lead antimonate was used as the colourant and an opacifier. Both samples also contain elevated Fe₂O₃ (1.80–1.81 %), which is quite common in lead antimonate-opacified glass, as iron increases the intensity of the colour (Molina et al. 2014, 182). Partly the depression in concentrations is due the diluting effect of the high lead and their reduced compositions (Table 4) have more typical Na₂O, SiO₂, and MgO values ($\bar{x} = 15.7\%$, 75.8 %, 0.41 %, respectively). However, reduced Al₂O₃ and CaO remain relatively low ($\bar{x} = 0.37\%$ and 3.73 %, respectively). One of the samples also contains traces of CuO (EPMA = 0.03%; LA-ICP-MS = 178 ppm), which is indicative of possible recycling, but could also have entered the glass with the lead antimonate.

Trace elements of this group have relatively weaker signal (Fig. 6) when compared to Na1, even allowing for the lead antimonate dilution. These characteristics, coupled with the very low Al₂O₃, may suggest a

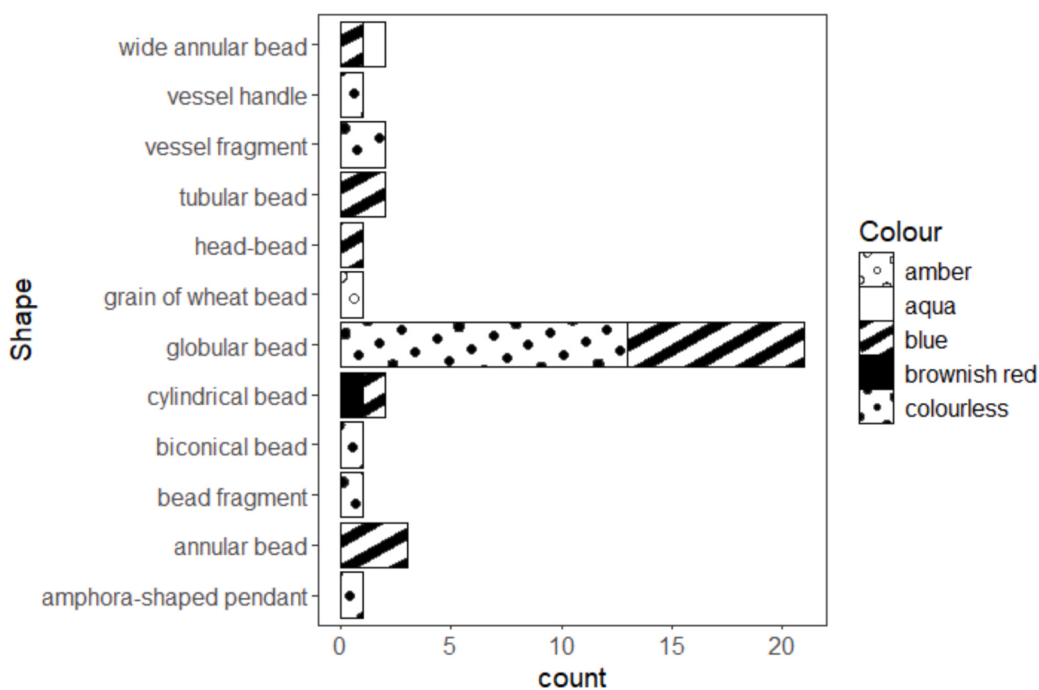


Fig. 3. Typology and colours of the analysed dataset.

glass made using vein quartz or pebbles as a source of silica, rather than sand.

Na3 ($n = 4$) comprises cobalt-coloured blue samples that have high Na₂O, MgO, and Al₂O₃ ($\bar{x} = 19.2\%$, 3.23 %, and 5.60 %, respectively), but low K₂O and CaO ($\bar{x} = 0.12\%$, 3.29 %, respectively). The high and positively correlated MgO and Al₂O₃, the former not typically encountered in natron-based glasses, are indicative of an alum cobalt source (Fig. 7). The glasses are coloured by c. 400 ppm cobalt (0.03–0.07 % CoO ($n = 4$, EPMA), $\bar{x} = 0.05$, $\sigma = 0.01$; 304–470 ppm ($n = 3$, LA-ICP-MS)), and cobalt concentrations in this group are on average lower than in the rest of the Co-coloured samples ($\bar{x} = 0.17\%$). Minor concentrations of MnO (0.21–0.27 %, $\bar{x} = 0.23$, $\sigma = 0.02$) and ZnO (0.03–0.07 % ($n = 4$, EPMA), $\bar{x} = 0.05$, $\sigma = 0.02$; 226–576 ppm ($n = 3$, LA-ICP-MS)) were also detected. Three samples from this group analysed by LA-ICP-MS, contain minor concentrations of Ni (357–497 ppm, $\bar{x} = 416$, $\sigma = 59.2$) but As, a characteristic marker of some cobalt ores, is present only in ultra-trace amounts (0.1–0.5 ppm).

Positive inflections of Zr and Cr (Fig. 6) may indicate the presence of chromite and zircon in the silica source. The concentrations of the REE are particularly high and diagnostic (Table 3): the heavy REE are enriched relative to the light REE, with a strong maximum around 0.31 for Sm and 0.40 for Eu (MUQ normalised). A strong correlation of yttrium with cobalt—the former generally considered to be a proxy for the heavy rare earth elements—indicates that the REE pattern is most likely a mixed signal, influenced by the strong and distinct colourant rather than characteristic of the silica source.

Na4 ($n = 3$) comprises glasses with Na₂O and Al₂O₃ averages typical of natron glasses ($\bar{x} = 15.7\%$, and 1.36 %, respectively), but low K₂O and CaO ($\bar{x} = 0.99\%$ and 3.68 %, respectively). TiO₂, P₂O₅ and Fe₂O₃ concentration are elevated ($\bar{x} = 0.15\%$, 0.17 %, and 10.2 %, respectively), while MgO is likewise elevated but highly variable ($\bar{x} = 2.47\%$, 0.87–3.54 %) (Figs. 5–6). Low concentrations of Sb₂O₅ (0.07 and 0.14 % (EPMA); LA-ICP-MS (Pu10) = 345 ppm) were detected in samples Pu10 and Pu17, the former also contains traces of CuO (0.04 % EPMA, 276 ppm LA-ICP-MS), and ZnO (0.04 % EPMA, 341 ppm LA-ICP-MS).

The samples are very weathered and, given their low CaO, likely would not have been preserved were it not for the high contents of Fe₂O₃ colourant (8.60–12.9 %). Elevated Fe₂O₃ could indicate use of sands

with high iron content, and the associated elevation of MgO might reflect the presence of Fe-Mg minerals. However, iron could also have been deliberately added, as scale or possibly slag which also may have carried elevated concentrations of magnesia. A single iron flake, potentially iron smithing scale was observed in one of the samples with high MgO (Pu17; Fig. 8), and iron working by-products have been observed in other early black glass (Eremin et al. 2012, Lončarić et al. 2024). However, further evidence is needed to draw any firm conclusions.

One sample (Pu10b) has lower MgO concentrations than the other two (Pu17b, Pu18b; MgO = 0.87 %, as opposed to 3.00–3.54 %) as well as lower CaO and Sr, but higher Fe₂O₃ (Figs. 5, 7). If the addition of iron-working by-products explains the colour, this may reflect the addition of a different slag material, as iron and lime (the latter derived from the ash) are typically major components of iron slag. The other minor and trace elements of the high- and low-MgO samples are otherwise broadly similar, suggesting a common source (Table 3).

The MUQ-normalised trace element pattern of black natron glass exhibits slightly positive Nb and Y inflections, but negative Ba, indicating the use of a different, impure type of sand (Fig. 6). The REE have a relatively high signal and, unlike almost all other examples in the dataset, show a distinctive negative Eu anomaly. Usually a feature of granites, this indicates a depletion in Eu²⁺-bearing plagioclase which sets the signal apart from glasses made using the plagioclase-bearing sands the eastern Mediterranean coast where the Eu anomaly is typically positive (Brems and Degryse 2014b: 78; Ceglia et al. 2019: 282; Phelps et al. 2016: 63; Wedepohl et al. 2011: 293). While the possibility that the large amounts of iron colourant affected the trace element pattern cannot be disregarded, there are no major differences in trace element patterns between sample Pu18b, with 9.1 % Fe₂O₃ and Pu10b with 12.9 % Fe₂O₃. Significantly, both black natron samples analysed for trace elements have notably high Li ($\bar{x} = 58.4$ ppm), Th ($\bar{x} = 3.5$ ppm) and U ($\bar{x} = 2.3$ ppm).

4.2. Group 2 – LMHK glass ($n = 2$)

Two blue copper-coloured samples have low Na₂O and CaO concentrations ($\bar{x} = 5.33\%$, and 2.30 %, respectively) as well as elevated

Table 2

EPMA results.

Sample	Na2O	MgO	Al2O3	SiO2	P2O5	SO3	Cl	K2O	CaO	TiO2	MnO	Fe2O3	CoO	CuO	ZnO	SnO2	Sb2O5	BaO	PbO	Total
GROUP 1																				
Na1																				
Pu1	15.79	0.56	2.07	70.37	0.07	0.21	0.83	0.78	7.27	0.05	bdl	0.39	bdl	bdl	bdl	bdl	1.58	0.03	bdl	100.00
Pu2	15.70	0.43	2.72	70.33	0.11	0.17	1.07	0.63	7.22	0.03	0.30	0.33	bdl	bdl	bdl	bdl	0.05	0.03	bdl	99.10
Pu4	16.23	0.54	2.18	68.66	0.06	0.41	0.91	0.51	8.08	0.04	bdl	0.39	bdl	bdl	bdl	bdl	1.99	bdl	bdl	100.00
Pu5	14.40	0.49	2.52	71.60	0.05	0.40	0.46	0.59	6.57	bdl	bdl	0.57	0.31	0.19	bdl	bdl	0.04	bdl	bdl	98.20
Pu6	15.01	0.58	2.54	67.97	0.26	0.41	0.24	1.79	8.01	0.05	bdl	0.45	bdl	0.03	bdl	bdl	1.05	bdl	bdl	98.40
Pu9	14.72	0.43	2.34	69.93	0.05	0.20	0.90	0.66	9.19	0.04	bdl	0.40	bdl	bdl	bdl	bdl	0.90	bdl	bdl	99.80
Pu11	16.63	0.46	2.53	68.27	0.09	0.14	0.98	0.75	6.94	bdl	0.02	0.29	bdl	bdl	bdl	bdl	0.04	0.02	bdl	97.20
Pu12	16.03	0.53	2.20	67.95	0.06	0.42	0.92	0.47	8.19	0.03	bdl	0.40	bdl	bdl	bdl	bdl	1.98	bdl	bdl	99.20
Pu14	17.27	0.47	2.59	69.88	0.10	0.11	0.98	0.78	7.17	bdl	0.01	0.30	bdl	bdl	bdl	bdl	0.03	bdl	bdl	99.70
Pu13b	16.68	0.51	2.65	65.51	0.05	0.47	0.89	0.58	7.84	0.09	0.32	0.71	0.12	0.19	bdl	bdl	1.20	bdl	bdl	97.10
Pu13w	17.01	0.50	2.42	66.72	0.04	0.41	0.94	0.62	7.94	0.07	bdl	0.55	bdl	0.03	bdl	bdl	1.66	0.03	bdl	98.90
Pu15	16.43	0.53	2.22	68.89	0.06	0.42	0.91	0.50	8.08	0.04	0.02	0.40	bdl	bdl	bdl	bdl	1.94	bdl	bdl	100.00
Pu19	14.56	0.58	1.83	70.32	0.08	0.32	0.58	0.68	6.52	0.05	bdl	0.47	bdl	bdl	bdl	bdl	2.31	0.04	bdl	98.30
Pu20	19.49	0.52	2.26	62.66	0.06	0.43	1.03	0.60	8.63	0.05	bdl	0.34	bdl	bdl	bdl	bdl	1.62	bdl	bdl	97.70
Pu21	16.91	0.35	2.28	60.05	0.03	0.33	1.01	0.45	6.37	0.06	bdl	0.54	bdl	0.03	bdl	bdl	1.64	bdl	10.26	100.00
Pu22	18.68	0.34	2.04	68.71	0.09	0.59	0.76	0.77	5.99	0.04	bdl	0.31	bdl	bdl	bdl	bdl	1.16	bdl	bdl	99.50
Pu23	16.41	0.44	2.47	70.17	0.06	0.32	0.91	0.65	7.23	0.03	0.05	0.73	0.11	0.19	bdl	bdl	0.05	bdl	bdl	99.80
Pu24	17.34	0.51	2.35	71.29	0.05	0.43	0.93	1.05	9.66	0.05	bdl	0.61	bdl	bdl	bdl	bdl	0.94	bdl	bdl	105.00
Pu25	13.07	0.51	2.11	68.43	0.08	0.40	0.64	0.62	9.80	0.04	0.12	0.79	0.06	0.10	bdl	bdl	0.04	0.04	bdl	96.90
Pu26	16.26	0.49	2.00	68.32	0.07	0.49	0.69	0.61	6.65	0.04	bdl	0.37	bdl	bdl	bdl	bdl	1.77	0.03	bdl	97.80
Pu27	12.55	0.58	2.23	68.99	0.14	0.24	0.64	1.04	7.58	0.04	0.25	0.81	0.11	0.17	bdl	bdl	0.09	0.04	0.04	95.50
Pu28	11.89	0.72	2.46	70.26	0.24	0.05	0.75	1.89	8.01	0.04	0.60	1.00	0.20	0.22	bdl	bdl	0.09	0.03	bdl	98.50
Pu30	16.70	0.43	2.04	66.48	0.08	0.60	0.62	0.73	6.80	0.03	bdl	0.31	bdl	bdl	bdl	bdl	1.20	0.03	bdl	96.10
Pu31	15.58	0.62	2.53	65.46	0.11	0.24	0.85	0.72	8.40	0.07	0.79	1.09	0.08	0.13	bdl	bdl	0.05	0.09	0.03	0.19
Pu33	16.46	0.53	2.24	69.18	0.05	0.41	0.93	0.46	8.11	bdl	bdl	0.39	bdl	bdl	bdl	bdl	1.94	bdl	bdl	101.00
Pu36	13.95	0.47	2.46	71.13	0.07	0.32	0.80	0.65	7.61	0.03	bdl	0.74	0.11	0.18	bdl	bdl	0.04	bdl	bdl	98.60
Pu38	16.97	0.50	2.14	67.39	0.10	0.59	0.68	0.78	8.84	0.04	bdl	0.34	bdl	bdl	bdl	bdl	1.07	0.03	bdl	99.50
Pu40	16.59	0.64	2.81	66.35	0.14	0.16	0.94	0.68	9.49	bdl	0.29	0.38	bdl	bdl	bdl	bdl	0.06	0.04	bdl	98.60
Na 2																				
Pu32y	9.73	0.25	0.24	47.85	bdl	0.20	0.38	0.10	2.39	bdl	bdl	1.81	bdl	bdl	bdl	bdl	3.77	bdl	32.59	99.30
Pu39y	10.33	0.28	0.24	49.27	0.03	0.25	0.41	0.13	2.39	bdl	bdl	1.80	bdl	0.03	bdl	bdl	3.67	31.71	101.00	
Na 3																				
Pu8	19.27	2.54	5.41	66.51	0.02	0.47	0.51	0.12	3.94	bdl	0.27	0.49	0.07	bdl	bdl	bdl	bdl	bdl	bdl	99.70
Pu32b	17.37	2.83	4.62	68.78	bdl	0.36	0.46	0.15	2.64	bdl	0.22	0.52	0.05	bdl	bdl	bdl	bdl	bdl	bdl	98.00
Pu37	20.38	3.71	6.33	64.24	bdl	0.46	0.58	0.10	3.04	bdl	0.22	0.66	0.04	bdl	bdl	bdl	bdl	bdl	bdl	99.80
Pu39b	19.97	3.83	6.04	63.43	bdl	0.43	0.51	0.11	3.55	bdl	0.21	0.64	0.03	bdl	bdl	bdl	bdl	bdl	bdl	98.80
Na 4																				
Pu10	15.26	0.87	1.56	65.41	0.13	0.14	0.36	1.11	2.43	0.17	0.03	12.91	bdl	0.04	0.04	bdl	0.07	bdl	bdl	100.50
Pu17	15.76	3.00	1.12	64.00	0.19	0.27	0.52	0.89	3.75	0.13	bdl	8.60	bdl	bdl	bdl	0.14	bdl	bdl	98.40	
Pu18	16.15	3.54	1.39	62.43	0.20	0.18	0.62	0.97	4.87	0.16	bdl	9.10	bdl	bdl	bdl	bdl	bdl	bdl	bdl	99.60
GROUP 2 – LMHK																				
Pu3	5.76	0.74	1.86	74.93	0.24	0.04	0.03	7.36	2.24	0.06	bdl	0.62	bdl	3.30	bdl	bdl	bdl	bdl	bdl	97.20
Pu7	4.89	0.72	1.73	78.09	0.23	0.05	0.02	7.26	2.35	0.07	bdl	0.57	bdl	2.10	bdl	bdl	bdl	bdl	bdl	98.10
GROUP 3 – PLANT ASH																				
Pu29	16.19	4.34	0.59	67.03	0.23	0.38	0.78	1.65	8.27	0.04	bdl	0.36	bdl	bdl	bdl	bdl	0.26	bdl	bdl	100.00
Pu34	14.23	3.07	0.71	70.41	0.16	0.34	0.55	1.08	6.60	0.07	0.16	0.49	bdl	bdl	bdl	bdl	0.60	bdl	bdl	98.50
oxides in wt%, Cl as element																				

Table 3
LA-ICP-MS results.

Sample	Pu3	Pu7	Pu8	Pu10	Pu13b	Pu13w	Pu14	Pu18	Pu20	Pu24	Pu29	Pu32b	Pu34	Pu39b	Pu39y
Li	35.9	38.8	6.3	36.5	3.8	4.0	3.2	80.2	3.0	3.1	5.9	3.6	4.9	4.2	1.4
Be	0.8	0.9	2.9	0.2	0.4	0.1	0.2	0.4	0.4	0.3	0.2	1.3	0.3	1.5	0.1
Na	45,124	38,654	151,236	113,041	137,330	138,502	126,034	127,903	158,504	142,456	125,788	136,310	113,677	156,801	77,159
Mg	4377	4091	14,616	4886	3319	3342	2847	20,673	3288	3307	25,138	17,152	18,520	20,980	1600
Al	9658	8392	27,960	7822	12,961	13,127	12,849	6797	11,765	11,668	2888	24,811	3686	30,970	1213
K	64,519	64,730	888	8942	4758	4953	6642	8291	5131	7052	14,474	1287	9322	856	1076
Ca	17,173	18,066	28,846	17,626	62,125	66,507	55,268	36,221	66,942	71,114	64,071	14,042	49,380	29,112	19,060
Sc	10.0	8.8	6.2	6.2	7.6	7.7	4.6	6.1	6.2	6.3	5.4	8.7	6.7	9.1	5.4
Ti	484	430	184	1123	558	573	326	1013	381	330	299	199	370	281	123
V	11.5	10.0	4.5	32.6	24.2	9.0	5.4	25.2	7.4	6.5	7.9	4.6	12.1	5.5	5.1
Cr	12.6	9.4	5.6	18.4	11.5	12.2	7.5	13.1	8.8	8.4	10.2	4.1	14.6	6.8	3.1
Mn	140	132	2124	282	4142	155	97	211	123	140	186	2197	1288	1722	31
Fe	5120	4631	4132	94,548	6501	4234	2460	66,548	2956	3014	3016	4056	3978	5317	13,629
Co	24.5	19.5	442	2.5	1541	2.6	1.1	2.1	1.9	2.8	1.3	470	2.2	304	0.8
Ni	60.7	46.8	394	14.5	240	4.4	3.1	9.6	3.4	2.7	7.9	497	9.7	357	3.1
Cu	25,993	16,569	15.7	276	2057	45.2	6.4	63.4	12.1	11.1	10.6	5.5	14.3	13.1	178
Zn	72.9	73.3	576	341	112	9.6	7.8	199	6.5	7.8	24.7	491	29.1	226	8.0
Ga	2.1	2.1	0.6	2.7	4.5	2.6	2.0	2.3	2.3	2.5	0.7	0.7	0.8	1.0	na
As	16.4	12.0	0.1	33.5	21.0	3.1	0.9	8.9	2.1	32.0	1.2	0.3	3.3	0.5	1437
Rb	92.6	82.8	1.2	15.9	9.0	9.2	9.5	16.4	7.9	11.4	7.3	0.8	4.9	1.0	1.6
Sr86	156	156	134	45.3	527	537	388	248	522	575	445	163	289	143	153
Sr88	167	166	144	46.2	522	526	396	256	519	570	438	169	288	150	161
Y	4.4	4.1	9.7	8.7	8.8	8.8	3.6	11.4	8.9	9.0	2.2	12.0	3.1	11.7	1.0
Zr	26.9	24.6	14.2	68.6	48.0	48.9	35.7	46.8	36.8	37.7	14.0	15.1	18.2	23.2	10.3
Nb	1.8	1.6	0.5	3.5	1.6	1.8	1.1	4.3	1.3	1.2	1.0	0.6	1.3	0.9	0.4
Mo	0.2	0.3	na	3.7	1.2	0.5	2.3	3.8	0.3	0.3	0.4	na	0.7	na	0.2
Sn	25.1	21.0	0.2	0.5	148	0.5	0.3	0.5	0.3	0.5	68.8	0.1	0.2	0.1	0.5
Sb	32.1	29.8	7.7	345	6962	13,473	0.3	11.5	12,581	8998	1659	18.8	4547	2.7	36,613
Ba	74.8	72.5	34.2	61.3	243	221	216	55.6	197	210	69.6	38.0	90.2	41.5	35.7
La	5.3	5.0	2.3	10.7	7.6	7.6	3.1	9.6	6.8	7.4	2.3	1.9	3.5	3.7	0.9
Ce	10.3	9.8	8.1	22.7	13.2	13.4	5.5	20.0	12.1	13.2	6.3	6.7	22.6	10.2	1.6
Pr	1.2	1.1	1.5	2.7	1.7	1.7	0.9	2.2	1.6	1.8	0.5	1.4	0.9	1.6	0.2
Nd	4.5	4.1	8.3	10.1	7.0	7.2	4.1	8.3	6.7	7.3	1.8	7.3	3.5	7.5	0.7
Sm	0.9	0.8	2.3	1.8	1.6	1.5	2.1	1.5	1.4	1.6	0.4	2.3	0.6	2.1	0.1
Eu	0.2	0.2	0.6	0.3	0.4	0.4	0.6	0.2	0.4	0.4	0.1	0.7	0.2	0.7	na
Gd	0.8	0.8	2.5	1.6	1.5	1.5	2.1	1.6	1.4	1.5	0.4	2.9	0.5	2.9	0.2
Tb	0.1	0.1	0.4	0.2	0.2	0.2	0.3	0.3	0.2	0.2	na	0.4	0.1	0.4	na
Dy	0.7	0.6	1.7	1.4	1.3	1.2	1.4	1.7	1.3	1.5	0.3	2.3	0.4	2.4	0.2
Ho	0.1	0.2	0.3	0.3	0.3	0.3	0.3	0.3	0.3	0.3	0.1	0.5	0.1	0.4	na
Er	0.4	0.5	0.7	0.8	0.8	0.8	0.9	1.0	0.7	0.8	0.2	1.2	0.2	1.1	0.1
Tm	0.1	0.1	0.1	0.1	0.1	0.1	0.2	0.1	0.1	0.1	na	0.2	na	0.1	na
Yb	0.5	0.4	0.6	0.7	0.7	0.6	1.2	1.0	0.6	0.7	0.1	0.9	0.2	0.9	0.1
Lu	0.1	0.1	0.1	0.1	0.1	0.1	0.3	0.1	0.1	0.1	na	0.1	0.0	0.1	0.0
Hf	0.7	0.6	0.3	1.6	1.0	1.2	1.2	1.1	0.9	1.0	0.3	0.2	0.4	0.4	0.2
Tl	na	na	na	0.1	na	na	0.4	na	na	0.1	na	na	na	na	0.1
Pb	31.0	26.1	13.1	260	86.3	105	10.5	2.5	13.1	90.6	3.7	27.2	2.9	7.6	325,342
Bi	na	na	na	0.1	na	na	0.4	na	na	0.1	na	na	na	na	na
Th	1.5	1.5	0.9	4.0	0.9	0.9	0.7	3.0	0.8	0.9	0.4	0.9	0.5	1.3	0.3
U	0.4	0.4	0.8	2.1	1.7	1.7	0.6	2.5	1.1	0.9	0.6	0.8	1.7	1.0	0.4

elements in ppm

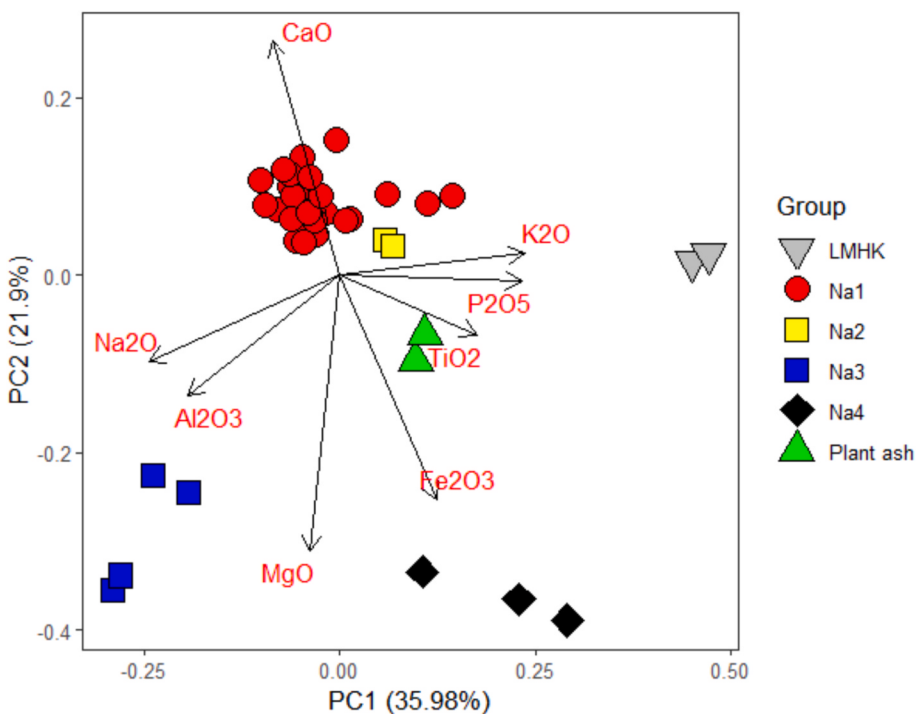


Fig. 4. PCA biplot using Principal Components 1 and 2, demonstrating the differences between plant ash, LMHK and four subgroups of natron glasses. The groups are created using base glass-related elements (Na_2O , MgO , Al_2O_3 , P_2O_5 , K_2O , CaO , TiO_2 , and Fe_2O_3). Analyses were performed using R (version 4.2.3, R Foundation for Statistical Computing, 2023), and the plots were generated using the ggplot2 package (version 3.3.5).

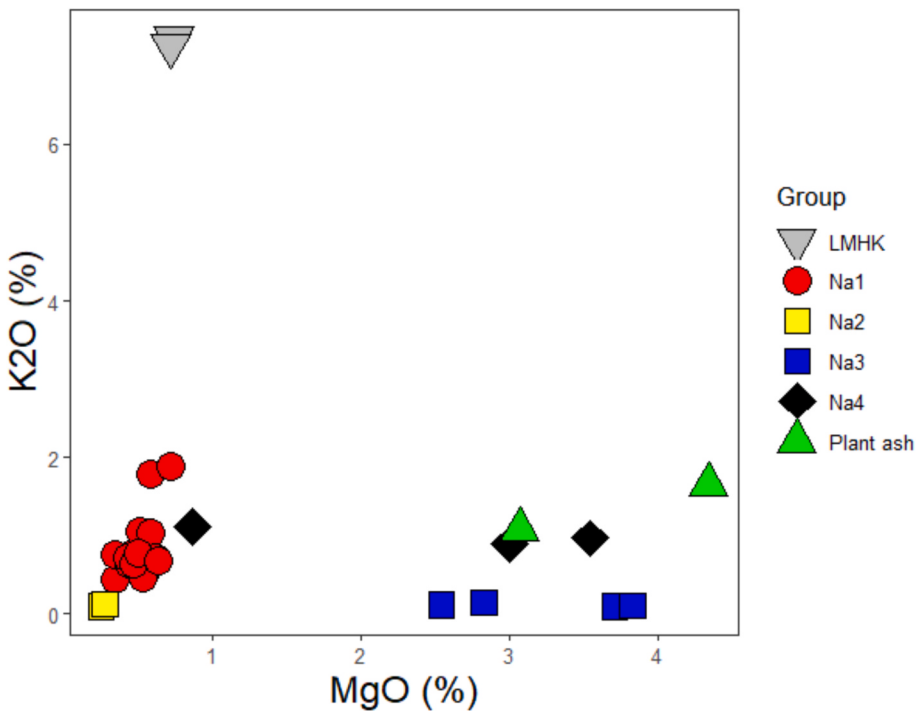


Fig. 5. Plot of MgO and K_2O in the studied samples confirms the compositional subgroups.

P_2O_5 and K_2O ($\bar{x} = 0.24\%$, and 7.31% , respectively). The elevated amounts of these oxides, as well as CaO concentrations which are too low for a plant ash flux signature, suggest the use of a mixed-alkali flux, seen in the Late Bronze Age mixed-alkali glasses (LMHK—low magnesium, high potassium; Henderson 1988; Venclová et al. 2011: 564). The group is also characterised by very high Rb which, in this case, is related

to the high potassium. The low amounts of Cr and Zr , and of other trace elements, indicate a relatively pure silica source, possibly vein quartz or quartz pebbles (Fig. 6). The two LMHK samples are coloured using Cu , which is present at 2.10 and 3.30% .

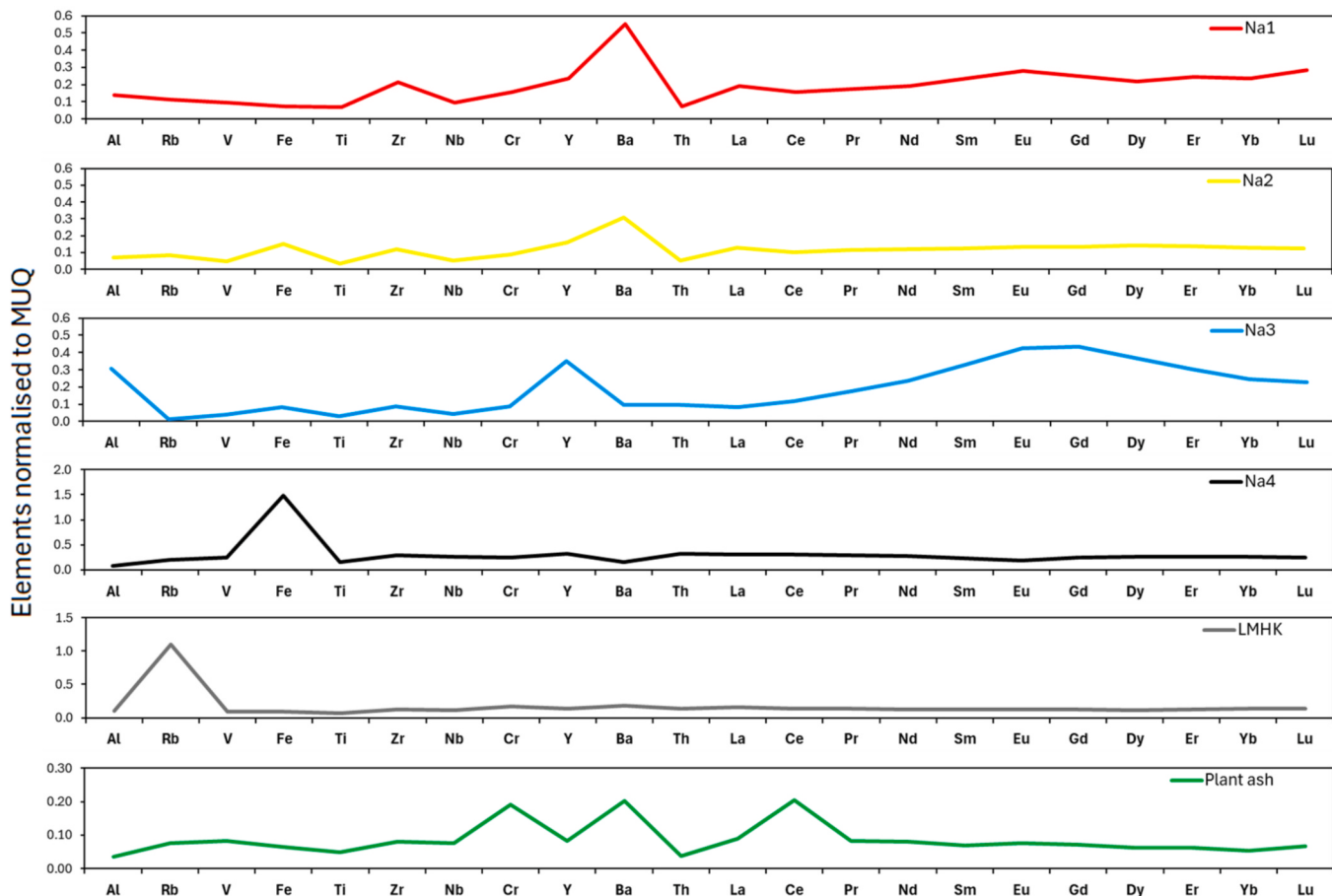


Fig. 6. Average trace elements of respective groups. Note the positive Ba anomaly in Na1, overall low signals of REE in the Na2, elevated REE in Na3, negative Eu anomaly in Na4, positive Rb anomaly in LMHK, and positive Ce anomaly in plant ash glass. Normalised to MUQ values from Kamber et al. 2005.

Table 4
Reduced mean major components of compositional groups.

Glass type	Number of samples	Na ₂ O*	MgO*	Al ₂ O ₃ *	SiO ₂ *	P ₂ O ₅ *	SO ₃ *	Cl*	K ₂ O*	CaO*	TiO ₂ *	MnO*	Fe ₂ O ₃ *	BaO*
Group 1														
Na1	28	16.3	0.52	2.41	70.0	0.09	0.36	0.83	0.77	7.99	0.04	0.12	0.54	bdl
Na2	2	15.7	0.41	0.37	75.8	0.02	0.35	0.62	0.18	3.73	bdl	bdl	2.82	bdl
Na3	4	19.4	3.26	5.65	66.4	0.01	0.43	0.52	0.12	3.32	bdl	0.23	0.58	bdl
Na4	3	15.8	2.48	1.36	64.3	0.17	0.20	0.50	1.00	3.70	0.15	0.03	10.3	bdl
Group 2														
	2	5.61	0.77	1.89	80.6	0.25	0.05	0.03	7.70	2.42	0.07	bdl	0.63	bdl
Group 3														
	2	15.4	3.74	0.66	69.5	0.20	0.36	0.67	1.38	7.51	0.06	0.08	0.43	bdl

*Reduced average compositions

4.3. Group 3 – Plant ash glass (*n* = 2)

Two samples, with a Na₂O average of 15.21 % and Al₂O₃ average of 0.65 % have elevated MgO, P₂O₅, and K₂O concentrations ($\bar{x} = 3.71\%$, 0.20 %, and 1.37 %, respectively), indicating that these were made with a halophytic plant ash flux. The low Al₂O₃ indicates a relatively pure silica source. The glasses display similar overall patterns of trace elements. The concentrations of trace elements controlled by the sand-source exhibit very low concentrations; most at levels less than 0.1 relative to the continental crust values. This is consistent with the use of a pure silica source (Fig. 6). Positive anomalies are observed for Cr and generally Ba, the latter likely related to ash. The REE pattern is fairly flat, but all samples show a very distinctive positive cerium anomaly.

The two samples have been intentionally decolourised with antimony (Sb₂O₅ 0.26–0.60 %, $\bar{x} = 1.5$, $\sigma = 0.5$); one of them also has elevated MnO (0.16 %), and could be a product of recycling.

5. Discussion

5.1. Natron glass

Na1. The composition of the dominant natron subgroup shows strong similarities with natron glass found across the Mediterranean from approximately the sixth century BCE to the ninth century CE. Its overall elemental concentrations resemble some other Early Iron Age natron glasses (Arletti et al. 2010; 2012; Braun 1983; Shortland and Schroeder 2009) (Fig. 9) and Hellenistic glasses (Oikonomou et al. 2020; Oikonomou 2018; Panighello et al. 2012; Paynter and Jackson 2019; Reade and Privat 2016), as well as later natron glasses known to have been made in primary production sites in Syria-Palestine such as Jalame and Apollonia (Freestone et al. 2000, 2003; Tal et al. 2004).

Low Zr and Ti (Zr < 50, Ti < 580 ppm) are suggestive of a Levantine, rather than Egyptian origin and it has been argued that high Sr is also indicative of the Levant (Rolland 2021), although some productions

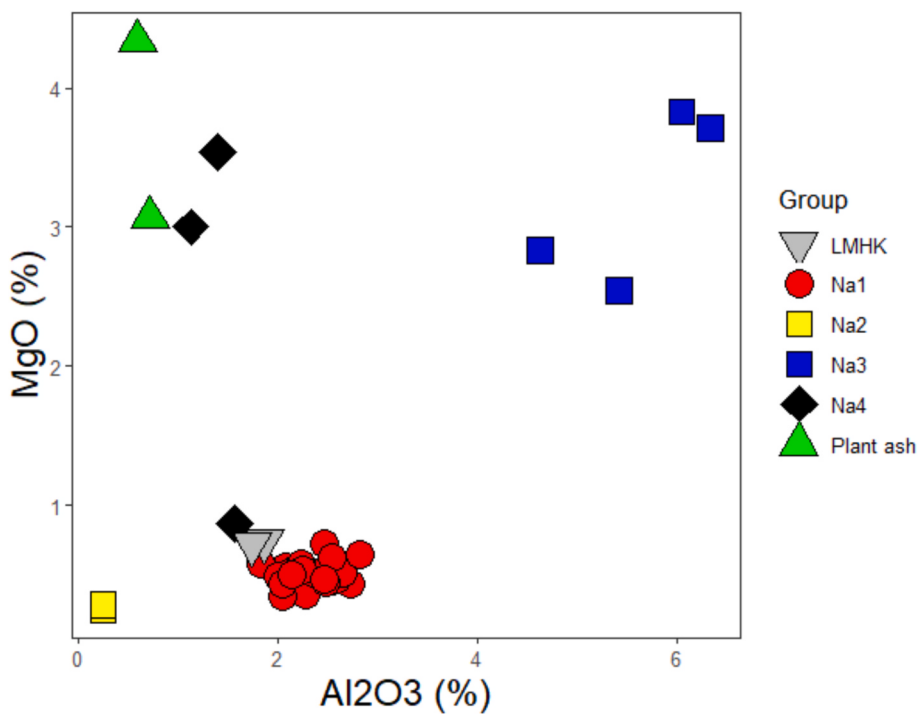


Fig. 7. Difference in MgO and Al₂O₃ in the recognised groups. Note the positive correlation of these oxides in the Na3 (cobalt alum) group.

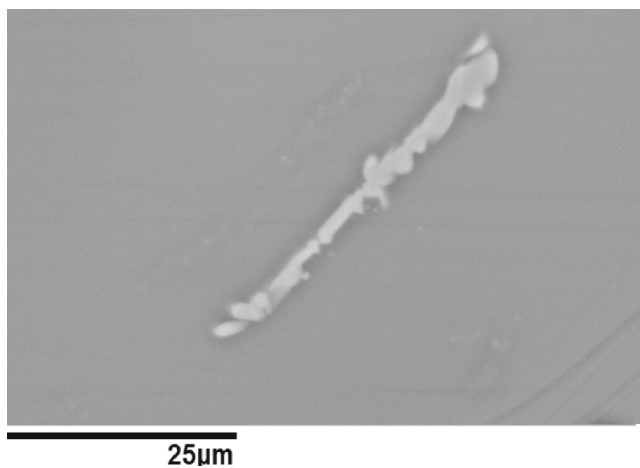


Fig. 8. Tentative iron scale in one of the Na4 samples (Pu17). Other than this inclusion, the glass matrix was homogenous.

such as Roman antimony-decolorised glass, generally accepted to be Egyptian (Barfod et al. 2020; Gliozzo 2017), also have high Sr. The trace element pattern, with a positive Eu anomaly, is also characteristic of Levantine coastal sands (Blomme et al. 2016, 2017; Degryse and Shortland 2009; Wedepohl et al. 2011). The similarity of compositions to the later Levantine (Roman) glass indicates trade of glass made in the Levant was already taking place by the sixth century BCE.

The majority of samples in this natron group is colourless ($n = 18$) and most contain high levels of Sb₂O₅ (0.9 – 2.31 %), typically around 1.5 % (Table 2), which suggests intentional decolorisation. Antimony was introduced as a decoloriser as early as the ninth century BCE, as indicated by the analysis of plant ash and possible natron glass from Nimrud, Iraq (Reade 2021). It is known as a decoloriser in glass from the Hellenistic world which is thought to have originated in the Levant, and which has Al₂O₃ and CaO contents close to those in our sample set (e.g. Oikonomou et al. 2020).

The background levels of manganese oxide in Mediterranean glass-making sands are generally up to 0.03 % (Brems and Degryse 2014a,b; Schibille et al. 2017; Brems et al. 2018) and manganese above these levels can be considered a deliberate addition. While in earlier periods Mn was used as a colourant to produce purple glass (e.g. Shortland and Eremin 2006), it was frequently used as a decoloriser from around the second century BCE (Henderson 2013; Sayre 1963). A number of glasses in the present assemblage contain MnO above background levels. However, MnO is present at around 0.3 % in one transparent glass (Pu2) where it is likely to have been added as a decoloriser, suggesting that this bead – dated to a broad range of 800–100 BCE – can be dated to the Late Iron Age. This sample also has trace amounts of Sb₂O₅ (0.05 %, no LA-ICP-MS data), suggesting recycling history, as well as Al₂O₃ at a somewhat higher level than the Sb-decolorised beads (c. 2.7 %) which is consistent with a slightly later origin; early Roman Levantine glasses can have Al₂O₃ contents at about this level (e.g. Thirion-Merle 2005; Freestone et al. 2025). Two transparent vessels (Pu11 and Pu14) also have somewhat high Al₂O₃ (c. 2.5 %) and contain no MnO above the background and only traces of Sb₂O₅ (0.03 – 0.04 %, no LA-ICP-MS data) – they also may represent later Iron Age Levantine glasses containing a little recycled earlier material.

Further tentative evidence of recycling can be observed in two antimony-decolorised samples (Pu6, Pu21) which have trace amounts of CuO (0.03 %, no LA-ICP-MS data). Furthermore, sample Pu6 contains elevated phosphorus and potassium, and low chlorine, which are all indicators of recycled glass (Barfod et al. 2018). Sample Pu21 is also characterised by the presence of 10.26 % PbO. The presence of small quantities of PbO in Hellenistic colourless glass (typically 1–4 %) is known for example from fourth century BCE Vergina (Brill 1994) and elsewhere (Paynter and Jackson 2019), but such a high level as seen here is rare. A possible explanation for this sample might involve the failure of a lead antimonate glass or a high-lead opaque white glass (e.g. Freestone and Stapleton 2015) but the interpretation is far from certain at this stage.

Sample Pu40 is amber in colour. It contains low Fe₂O₃ (0.38 %), moderately elevated Sb₂O₅ and MnO (0.06 % (no LA-ICP-MS data) and 0.29 %, respectively), and generally similar chemical composition as the

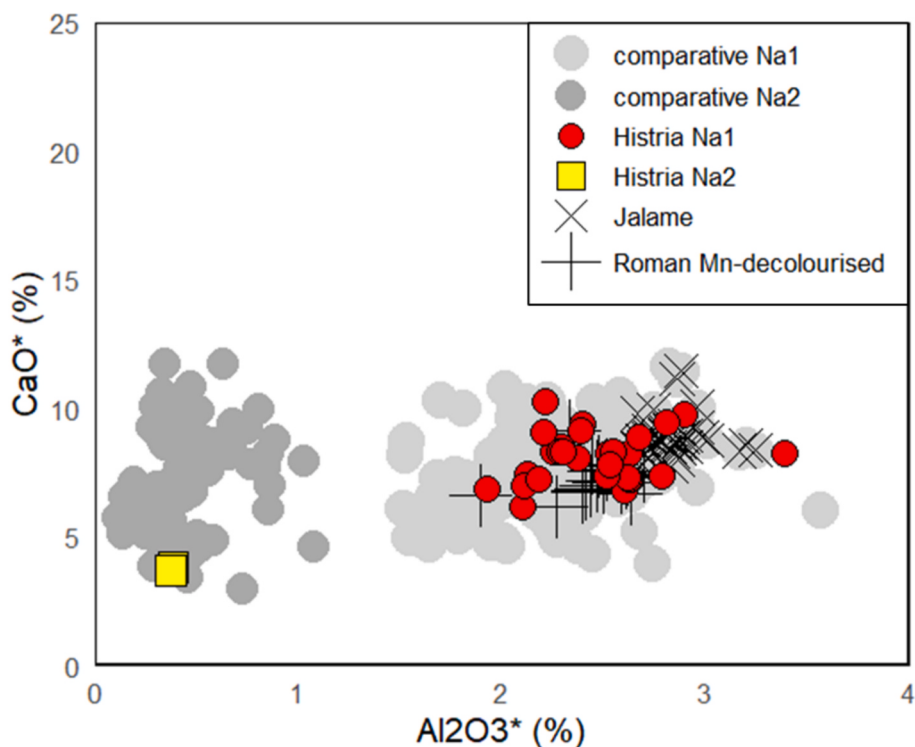


Fig. 9. Reduced CaO and Al₂O₃ in the Na1 and Na2 groups plotted alongside analogous examples. Comparative data for Na1 from Arletti et al. 2010, 2012; Braun 1983; Freestone et al. 2023; Oikonomou 2018; Panighello et al. 2012; Paynter 2008; Reade and Privat 2016; Shortland and Schroeder 2009. Comparative data for Na2 from Braun 1983; Conte et al. 2016, 2019; Franjić et al. 2022; Tzankova and Mihaylov 2019; Yatsuk et al. 2024a,b.

translucent glass, indicating the amber colour was achieved through a charge transfer between ferric iron and sulfide ions in reducing conditions (Schreurs and Brill 1984; Möncke et al. 2014: 33).

The rest of the samples in Group Na1 ($n = 8$) are blue; they contain elevated amounts of Fe₂O₃ (0.6–1.1 %), CoO (0.1–0.3 %, $\bar{x} = 0.1\%$, $\sigma = 0.1$) as well as CuO (0.1–0.2 %, $\bar{x} = 0.2\%$, $\sigma = 0.04$). The two latter oxides exhibit a positive correlation in most of the samples, indicating these are coming from the same cobalt ore source. The cobalt blue glasses contain MnO ranging from background level to 0.9 %. This is likely to indicate that in the later Iron Age, cobalt was added to glass which had already been decolourised, probably at the primary glass-making stage (cf. Freestone et al. 2023) and that the blue glasses with high MnO postdate those with low MnO. The relative chronology for most of these samples, retrieved from the dual cremation grave in Mariškići dated to 300–100 BCE, also supports this. These blue glasses also contain small amounts of Sb₂O₅ (0.04–0.09 %); this is likely to reflect recycling and could indicate the use of opaque blue glass as a source of cobalt. Elevated P₂O₅ and K₂O in samples Pu27b and Pu28b are also indicators of recycling.

The only blue sample of Group Na1 with trace elemental data (Pu13b) has elevated Ni (240 ppm), As (21 ppm), Zn (112 ppm), Cu (2057 ppm) Sb (6962 ppm) and Sn (148 ppm). Its CoO/NiO ratio (6.4) is lower than the range of 24–54 encountered in Hellenistic/Roman cobalt sources (Gratuze et al. 2018: 225). The decoration of this bead (Pu13w) is also the only example of opaque white-coloured glass in this assemblage and contains elevated Sb₂O₅ (1.66 %). The amount of CaO (7.94 %) in this sample does not differ from the CaO amount in other glasses from the same group ($\bar{x} = 7.79\%$, $\sigma = 1.4$), suggesting Sb₂O₅ rather than Ca₂Sb₂O₇ was added to the glass batch (Shortland et al. 2018: 778, Lahil et al. 2008: 109; 2009: 574; 2010: 688).

Na2. Low alumina concentrations (below 1 %) similar to those seen in this subgroup, have been reported in many published datasets for prehistoric natron glasses (cf., among others, Arletti et al. 2012; Braun 1983; Conte et al. 2016, 2018, 2019; Gratuze 2009; Oikonomou et al.

2016; Panighello et al. 2012; Paynter and Jackson 2019; Reade et al. 2005; Šmit et al. 2020; Towle and Henderson 2004; Tzankova and Mihaylov 2019; also see Type 0 in Lü et al. 2021). South Italian natron glasses from Sarno, Capua, and Francavilla Marittima, analysed by Conte et al. (2016, 2019), and dated to the ninth to sixth century BCE, as well as low-Al glasses from Novo Mesto (Franjić et al. 2022), are the closest compositional match to the Histrian examples (Fig. 9).

A single LA-ICP-MS analysis indicates a very low concentration of Zr at c. 10 ppm, which is lower than in the LBA glasses from Tel el Amarna ($\bar{x} = 30$ ppm) known to have been made from crushed quartz (Rehren and Pusch 2008; Shortland and Eremin 2006). Since these samples from Picugi are among the oldest in the assemblage (1000–600 BCE), it is on balance most likely the glass used for the yellow decoration are made with vein quartz, or pebbles derived from vein quartz, representing a continuation of the LBA glassmaking tradition. At present, it is clear that the presence of low-alumina natron glass in various regions during the first millennium BCE – or at least during its first half – indicates the existence of a distinct production centre, which was producing glass and/or glass items for a wider geographical area.

Na3. The combination and correlations of elements in subgroup Na3 type (Figs. 4, 6, 7, 10) indicates use of cobalt alum derived from the Western Oasis in Egypt (Gratuze 2009; Gratuze and Picon 2005: 11; Kaczmarczyk 1986; Reade et al. 2005; Reade 2021; Shortland et al. 2006). Compositionally, these Istrian glasses also closely resemble coeval alum-coloured beads from Mesopotamia, France, and Italy (Arletti et al. 2011; Gratuze and Picon 2005; Yatsuk et al. 2023a,b; Brill 1999) (Fig. 10). The positive correlation between MgO and Al₂O₃ reflects the cobalt alum pigment source and indicates that the base sands may have been low in both of these components. Despite the pronounced differences in elemental composition of Na3 and Na2 arising from the colourant addition, similarities in elements such as K, Ca, Sr, Ba and Zr could point to the same workshop.

Na4. The low lime and alumina in subgroup Na4 suggest a sand source with fewer feldspars and relatively low calcite. These traits are

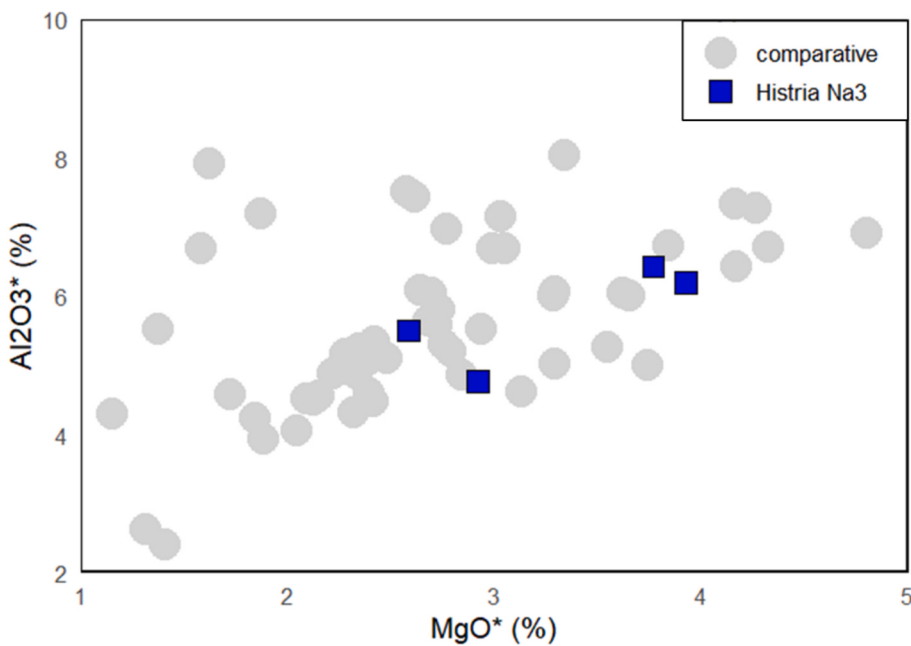


Fig. 10. Comparison of Na3 glasses from Histria with alum-coloured samples from France, Italy, and Mesopotamia (comparative data from Arletti et al. 2011; Brill 1999; Gratuze and Picon 2005; Reade 2021; Yatsuk et al. 2023a).

usually diagnostic of early natron glasses whose recipe has not yet been consolidated, and the combination would result in a less stable glass if the iron oxide amounts were not as elevated (Conte et al. 2018: 515; Reade et al. 2009: 53). The average ratio of MgO and CaO is 0.7, indicative of dolomitic rocks (Yatsuk et al. 2024b: 6).

Two samples analysed by LA-ICP-MS have higher zirconium than the other glasses (46 and 69 ppm). High zircon is associated with Egyptian

glass making sands (Foy et al. 2003; Shortland et al. 2007: 788). However, in the present case the high Li contents appear to rule out an Egyptian origin (e.g. Shortland et al. 2007 for LBA Egyptian glass, Freestone et al. 2018; Schibille et al. 2019 for later glasses). In the Zr/Ti vs Cr/La diagram (Fig. 14), useful for discriminating between Egyptian and Mesopotamian sands (Shortland et al. op. cit.), the black glasses are in an area of overlap, allowing an origin in either region. The major

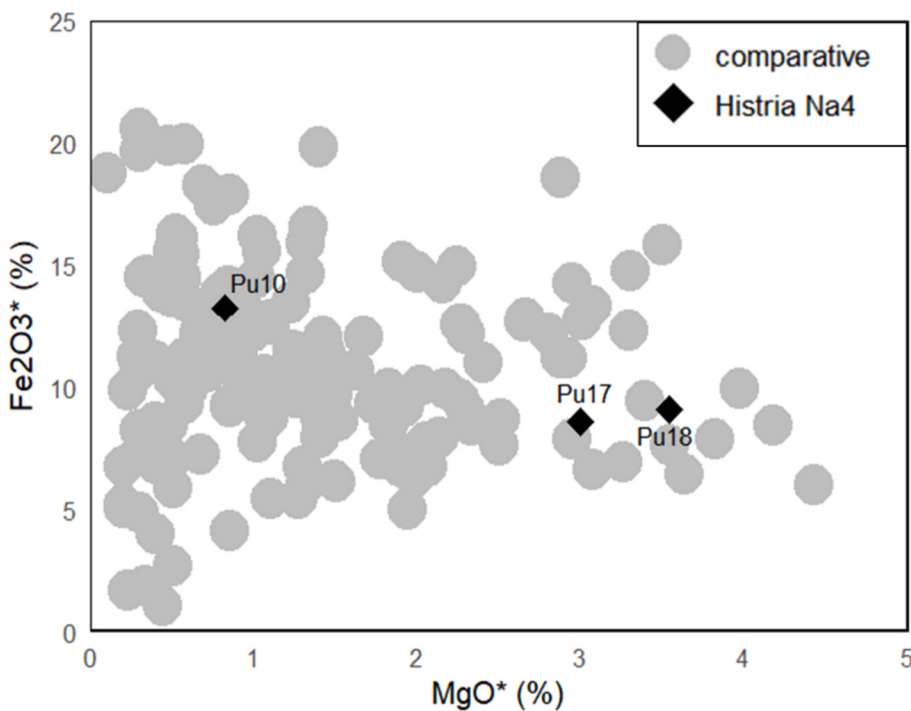


Fig. 11. First-millennium BCE black natron glasses. Difference in concentrations of MgO suggests more than one source of black natron glass. The samples from the dataset (Na4) most closely resemble examples from South and Central Italy, Pella, and Hasanlu. Additional data from Arletti et al. 2010, 2011 (Bologna); Braun 1983 (Westiran, Byčí skála, Ialyssos); Brill 1999 (Hasanlu Tepe); Conte et al. 2016 (Sarno, Cuma); 2018 (Pozzouli, Cuma, Bologna); 2019 (Francavilla Marittima, Torre Galli); Eremín et al. 2012 (Carthage); Reade et al. 2009 (Pella); Tzankova and Mihaylov 2019 (Dren-Delyan); Yatsuk et al. 2024 (Bisenzio, Marino, Roma, Sermoneta, Veio).

element compositions of the Na4 samples show similarities with other black glass from various Early Iron Age sites (Arletti et al. 2010, 2011; Brill 1999; Conte et al. 2018, 2019; Eremin et al. 2012; Reade et al. 2009; Reade 2021; Tzankova and Mihaylov 2019; Yatsuk et al. 2024b) (Fig. 11). However, some examples from South and Central Italy, Bulgaria, and Jordan have elevated MgO, while some comparative black natron glasses do not, suggesting a range of MgO concentrations, and some variability in this unconsolidated early natron glass type, perhaps relating to the way iron oxide entered the batch. In the case of the central Italian glasses with a similar trace element fingerprint, iron-bearing deposits have been suggested as the source of elevated iron (low Ba group of Yatsuk et al. 2024b).

The negative Eu inflections and the high Li, Th and U in the black glasses is different from the signature of eastern Mediterranean sands usually encountered in natron glasses. This trace elemental pattern, and in particular the elevated amounts of Li, Th and U (Table 3, Fig. 12) shows remarkable similarities to the glasses from Pella and southern and central Italian samples, allowing to presume a similar provenance for our samples from the Pula cemetery. High boron contents measured in the samples from Sardis (Van Ham Meert et al. 2019), point to a tentative Anatolian origin, but unfortunately B was not analysed in the present case, nor in the samples from Pella.

5.2. Group 2 –LMHK

Two mixed-alkali glass beads from the Lim hillfort cemetery are among the oldest in the assemblage (tenth to ninth century BCE). The overall fingerprint of these beads conforms closely to the LMHK Fratessina and related glasses (Fig. 13), and can most likely be considered a local North Italian product of LBA Fratessina workshops (Angelini et al. 2004; 2009; Towle et al. 2001; Venclová et al. 2011; Bettineschi et al. 2021).

The local European provenance of the studied beads can also be hypothesized on the basis of typology, as they are of the so-called *Pfahlbauperlen* type (also: *Pfahlbauönnchen*): a barrel-shaped bead most frequently found in lake dwellings in Switzerland but also in France, Italy, Austria, Czech Republic, Germany, and Belgium, with a

few examples also retrieved in Greece and Turkey (Billaud and Gratuze 2002; Cosyns et al. 2005: 323; Hartmann et al. 1997; Haevernick 1978: 148–156; Nikita and Henderson 2006; Towle et al. 2001; Venclová et al. 2011: 563; Yatsuk et al. 2023a).

5.3. Group 3 –Plant ash glass

The group of plant ash glasses shows marked compositional similarity with the Italian and Georgian Iron Age plant ash glass (Conte et al. 2016; Vachadze and Gratuze 2025; Yatsuk et al. 2024a), as they all share the positive Ce anomaly. Tentative Italian origin was suggested for the central Italian samples (Yatsuk et al. 2024a: 129) and possibility of Anatolian source of evaporitic deposit for the Georgian samples (Vachadze and Gratuze 2025: 9). It is our opinion that the trace-element concentrations of Group 3 show these plant ash glasses probably belong to the LBA Mesopotamian tradition (Fig. 14); the higher Cr/La ratio suggests Mesopotamian, chromite-bearing sands as opposed to Egyptian, zircon-enriched silica sources (Shortland et al. 2007: 788).

5.4. General implications

Although the overall frequency of some of the compositional groups encountered is relatively low, there appear to be associations with specific archaeological contexts. Both LMHK beads come from two different grave units (1100–1000 BCE) at the Lim hillfort, suggesting trade networks between the hillfort and the nearby Veneto region. Similarly, the black natron-type glass (Na4) was identified exclusively in the Pula cemetery (beads dated 1000–500 BCE). Natron glass with low alumina (Na2) and three alum-coloured samples (Na3) were retrieved from Picugi, while the fourth alum-coloured sample was found in Nesactium (beads dated 1000–600 BCE). All of these sites were in use from the Late Bronze Age onwards (twelfth century BCE–), and show how the early natron types readily reached the eastern Adriatic soon after their inception. Furthermore, the association with specific contexts suggests that the flow of glass beads into the region was not continuous, but perhaps a result of isolated events involving specific individuals or episodes of exchange.

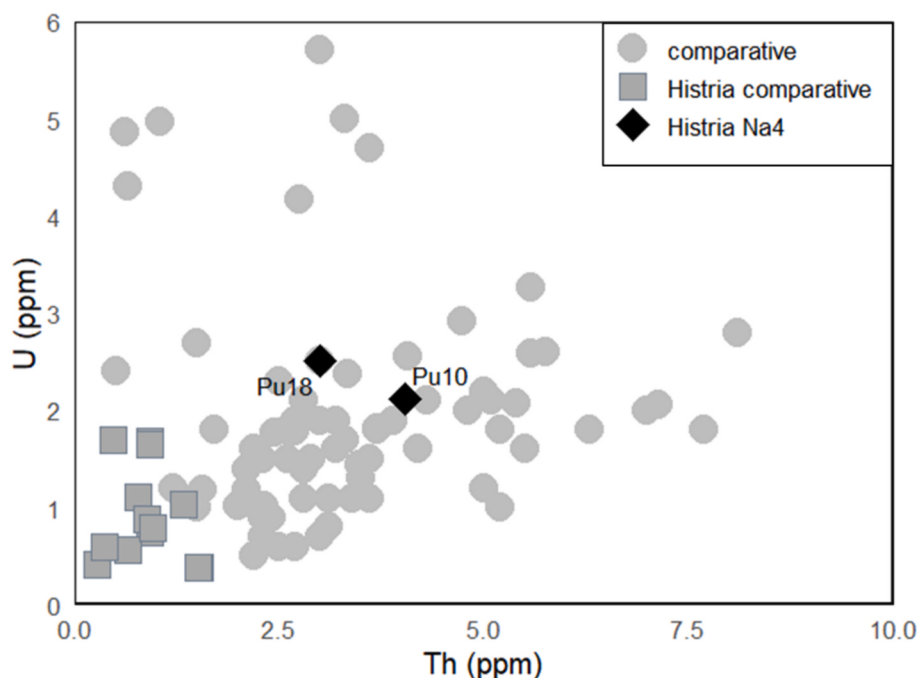


Fig. 12. Elevated concentrations of Th and U in Na4 type from Histria is remarkably similar to the Pella and Italian black natron glasses and confirms their similar provenance. Additional data from Arletti et al. 2011 (Bologna); Conte et al. 2016 (Cuma, Sarno), 2018 (Bologna Fair, Pozzuoli), 2019 (Francavilla Marittima, Torre Galli); Reade 2021 (Pella); Yatsuk et al. 2024 (Bisenzio, Marino, Roma, Sermoneta, Veio).

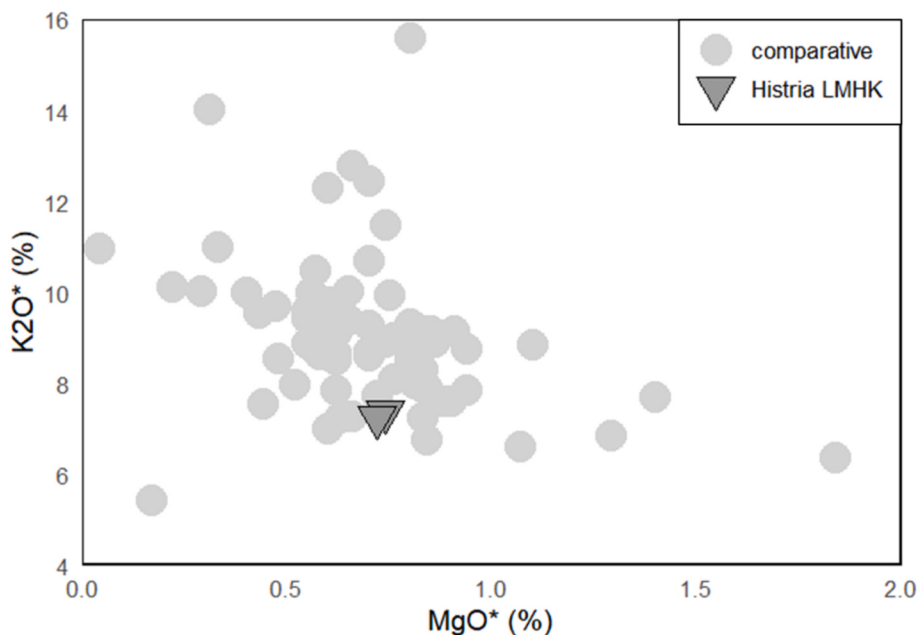


Fig. 13. MgO and K_2O concentrations in mixed-alkali samples correspond to the concentrations in LMHK glass, thought to originate in northern Italy. Comparative data from Angelini et al. 2004 (Frattesina); Brill 1992 (Frattesina); Conte et al. 2016 (Broglio di Trebisacce, Lipari-P. Monfalcone, Roca Vecchia); Towle and Henderson 2004 (Mariconda, Frattesina); Venclová et al. 2011 (Bohemia).

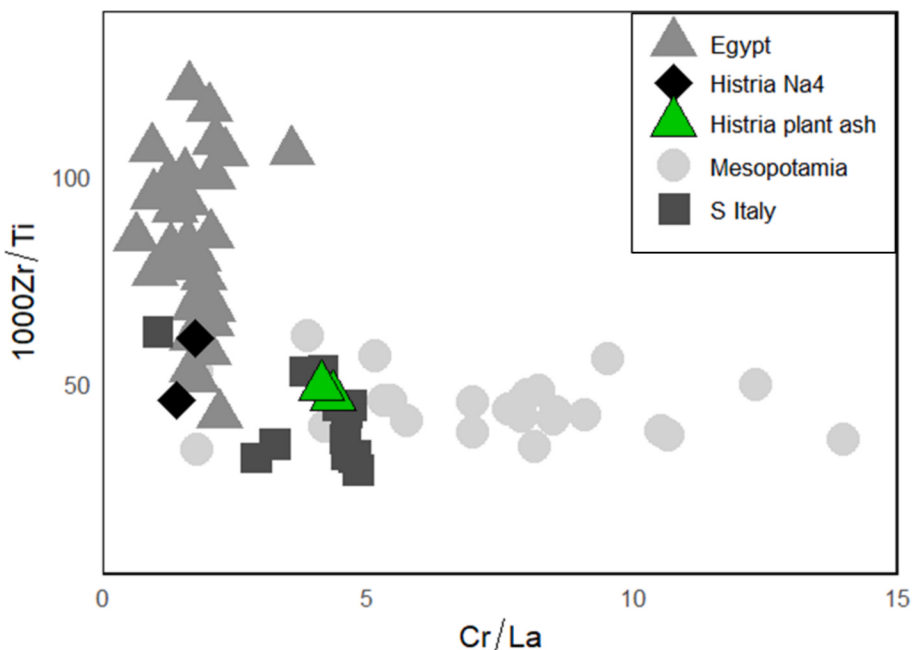


Fig. 14. Ratio of sand-related trace elements in plant ash glass resembles the pattern of Late Bronze Age Mesopotamian glasses, as well as samples from South Italy. Black natron from present study is in an area of overlap. Comparative data from Conte et al. 2016 (Sarno); Shortland et al. 2007 (Nuzi); Shortland 2012 (Amarna).

The yellow glasses of subgroup Na2 occur as decoration on the cobalt-blue glasses of subgroup Na3. Superficially there is some similarity in these two natron groups which both show particularly low K_2O and CaO relative to most natron glass in their reduced compositions (Table 4). This may suggest that the glasses of the same base composition were coloured in the same workshop, - and, if the elements such as the REE—which are likely to have been added with the colourants—are excluded, the limited remaining trace elements (i.e. Sr, Zr, Nb, Cr, Ba) are consistent with this view. More data on coexisting colours would be helpful to investigate this issue further.

The sixteen blue glasses analysed also offer an interesting cross-section of the first millennium BCE blue colourants found in Histria, as each colourant seems to be related to a distinct base glass (sub)type. The earliest, mixed-alkali glasses, are coloured with copper; ninth- to eight-century BCE glasses are coloured with cobalt-alum; and later natron glasses are coloured with a copper-rich cobalt colourant.

While the small number of plant ash glasses could suggest that these were heirlooms from the LBA, there is evidence of plant ash glasses still being produced during the Early Iron Age, and through to medieval times, in Mesopotamia, Syro-Palestine, and central Anatolia, and traded

in Europe (Conte et al. 2016; Henderson et al. 2018: 77; Reade et al. 2005; Reade et al. 2009: 51; Sayre and Smith 1961: 1852). Hence the scarcity of finds might be related to the distance involved, or the weaker trade network(s), perhaps related to the dominance of maritime over continental routes for trading.

6. Conclusion

The amount of glass from prehistoric Histria recovered from burials is likely to be an under-representation, as some items were likely lost during the cremation as well as during the transfer from the *ustrinum*, where the cremation was taking place, to the burial site. Overall, however, considering the size and time span of the region's sites, it can be said that the number of glass items is scarce, and they are certainly much less frequent when compared to the neighbouring regions, such as Lower Carniola.

On the other hand, the diverse chemical compositions encountered on the Histrian territory during the first millennium BCE echo the cross-cultural connections and close relationships of Histrian communities with the neighbouring regions. The earliest documented glass on the Histrian territory is the locally produced European LMHK glass, confirming contacts and trade exchange with Po valley workshops from very early on. Furthermore, the occurrence of early natron types from the eastern Mediterranean, such as the alum-coloured and low alumina beads, rarely found in the European archaeological record, indicate that Histrian communities had immediate access to novel technologies arriving from the East. The overwhelming presence of the consolidated natron type made in the Levant indicates continuing strong links with the long-distance trading networks and the emerging trade ports in the surrounding area.

The overall pattern of compositional types found in Histria is similar to those found in Italy, Slovenia, and other Iron Age communities of southern Europe. Frustratingly, although we have relatively precise origins for the Na1 Levantine group and the Frattesina-type glasses (Group 2), the origins of other widespread types – low alumina natron (Na2), alum-coloured natron (Na3), black natron (Na4), and even the “Mesopotamian” plant ash glasses (Group 3) are obscure and await further research.

How the glass reached the Histrian territory can only be conjectured. However, the geographical (and cultural) vicinity to major Etruscan trade centres, along with the later presence of Greek emporia on the Italian coast, suggest a tentative trade node for the flow of Mediterranean glass import to Histria. Similar compositional types (plant ash, mixed alkali, black natron, alum-coloured), found throughout Italy, as well as similar routes of some other imported prestigious goods, could also be taken to confirm this path from the Mediterranean into the eastern Adriatic via southeast Italian trade emporia.

CRediT authorship contribution statement

Ana Franjić: Writing – review & editing, Writing – original draft, Resources, Project administration, Methodology, Investigation, Funding acquisition, Formal analysis, Data curation, Conceptualization. **Ian C. Freestone:** Writing – review & editing, Validation, Supervision, Methodology. **Gry Barfod:** Writing – review & editing, Validation, Methodology. **Ulrike Sommer:** Writing – review & editing, Supervision. **Patrick Degrise:** Writing – review & editing, Funding acquisition.

Declaration of Competing Interest

The authors declare that they have no known competing financial interests or personal relationships that could have appeared to influence the work reported in this paper.

Acknowledgements

This research wouldn't have been possible without the expertise and kind help from Dr. Kristina Mihovilić, who allowed AF to access and sample the collections of the Archaeological Museum of Istria. She has indebted the archaeological community with her seminal work on the prehistory of northern Adriatic, and was supposed to be a co-author of this research. We would like to dedicate this paper to her memory (Kristina Mihovilić, 1951–2022).

The research was conducted as a part of a PhD project at the UCL Institute of Archaeology funded by an LAHP Studentship award to AF. This work was also supported by the Special Research Fund (BOF-KUL) C1 (Grant No. C14/19/060 and C16/24/004). The authors would like to thank the Archaeological Museum of Istria for allowing us to access and sample the artefacts, Tom Gregory for helping with the EPMA analysis, and the Society for Archaeological Sciences for providing a grant to conduct the LA-ICP-MS analysis at Aarhus University. Lastly, we would like to thank the reviewers of this article for their helpful comments and suggestions.

Appendix A. Supplementary data

Supplementary data to this article can be found online at <https://doi.org/10.1016/j.jasrep.2025.105368>.

Data availability

Data will be made available on request.

References

- Adlington, L.W., 2017. The Corning Archaeological Reference Glasses: New Values for “Old” Compositions. *Papers from the Institute of Archaeology* 27, Art 2, 1–8.
- Amoroso, A., 1885. I castellieri istriani e la necropoli di Vermo presso Pisino. *Atti e Memorie Della Società Istriana Di Archeologia e Storia Patria* 1.
- Amoroso, A., 1889. Le necropoli preistoriche dei Pizzughi. *Atti e Memorie Della Società Istriana Di Archeologia e Storia Patria* 5, 225–261.
- Angelini, I., Artioli, G., Bellintani, P., Diella, V., Gemmi, M., Polla, A., Rossi, A., 2004. Chemical analyses of Bronze Age glasses from Frattesina di Rovigo, Northern Italy. *J. Archaeol. Sci.* 31, 1175–1184.
- Angelini, I., Polla, A., Giussani, B., Bellintani, P., Artioli, G., 2009. In: Final Bronze-Age Glass in Northern and Central Italy: Is Frattesina the Only Glass Production Centre?. *Université Laval, Québec*, pp. 329–337.
- Arletti, R., Maiorano, C., Ferrari, D., Vezzalini, G., Quartieri, S., 2010. The first archaeometric data on polychrome Iron Age glass from sites located in northern Italy. *J. Archaeol. Sci.* 37, 703–712.
- Arletti, R., Bertoni, E., Vezzalini, G., Mengoli, D., 2011. Glass beads from Villanova excavations in Bologna (Italy): an archaeometrical investigation. *Eur. J. Mineral.* 23, 959–968.
- Arletti, R., Ferrari, D., Vezzalini, G., 2012. Pre-Roman glass from Mozia (Sicily-Italy): the first archaeometrical data. *J. Archaeol. Sci.* 39, 3396–3401.
- Baćić, B., 1958. Novi ilirski žarni grobovi u Puli. *Jadranski Zbornik*. 3, 315–322.
- Barfod, G.H., Freestone, I.C., Lichtenberger, A., Raja, R., Schwarzer, H., 2018. Geochemistry of byzantine and Early Islamic glass from Jerash, Jordan: Typology, recycling, and provenance. *Geoarchaeology* 33, 623–640.
- Barfod, G.H., Freestone, I.C., Lesher, C.E., Lichtenberger, A., Raja r., 2020. Alexandrian' glass confirmed by hafnium isotopes. *Sci. Rep.* 10, 11322.
- Barfod, G.H., Feveile, C., Sindbæk, S.M., 2022a. Splinters to splendours: from upcycled glass to Viking beads at Ribe, Denmark. *Archaeological and Anthropological Sciences* 14, 180.
- Barfod, G.H., Freestone, I.C., Jackson-Tal, R.E., Lichtenberger, A., Raja, R., 2022b. Exotic glass types and the intensity of recycling in the northwest Quarter of Gerasa (Jerash, Jordan). *J. Archaeol. Sci.* 140, 10546.
- Benussi, B., 1927. Dalle annotazioni di Alberto Puschi per la carta archeologica dell'Istria. *Archeografo Triestino* 14, 245–282.
- Betic, A., 2005. La necropoli dei Pizzughi. *Scavi Marchesetti (1904–1906, 1908–1909, 1913)*. In: Bandelli, G., Montagnari, G., Kokelj, E. (Eds.), Carlo Marchesetti e i castellieri 1903–2003. *Atti Del Convegno Internazionale Di Studi, Castello Di Duino (Trieste), 14–15 Novembre 2003. Fonti e studi per la Storia della Venezia Giulia IX*. Editreg, Trieste, pp. 591–612.
- Bettineschi, C., Angelini, I., Gratuze, B., 2021. Sulle tracce dei più antichi vetri dell'Altopiano dei Sette Comuni Vicentini. In: Burigana, L., Bettineschi, C., Magnini, L. (Eds.), *Traces of Complexity: Studi in Onore Di Armando De Guio = Studies in Honour of Armando De Guio*. Quingentole, SAP Società Archaeologica, pp. 261–278.

- Billaud, Y., Gratuze, B., 2002. Les perles en verre et en faïence de la Protohistoire française. In: Guialine, J. (Ed.), Matériaux, Productions, Circulation, Du Néolithique à L'âge Du Bronze. Errance, Paris, pp. 193–212.
- Bломме, А., Elsen, J., Brems, D., Shortland, A., Dotsika, E., Degryse, P., 2016. Tracing the primary production location of core formed glass vessels, Mediterranean Group I. *J. Archaeol. Sci. Rep.* 5, 1–9.
- Bломме, А., Degryse, P., Dotsika, E., Ignatiadou, D., Longinelli, A., Silvestri, A., 2017. Provenance of polychrome and colourless 8th–4th century BC glass from Pieria, Greece: a chemical and isotopic approach. *J. Archaeol. Sci.* 78, 134–146.
- Braun, C., 1983. Analyse von Gläsern aus der Hallstattzeit mit einem Excurs über römische Fenstergläser. In: Haevernick, T., Frey, O.H. (Eds.), Glasperlen Der Vorrömischen Eisenzeit Vol.i. Marburger Studien Zur Vor- Und Frühgeschichte; Bd.5. Verlag Phillip von Zabern, Mainz am Rhein, pp. 129–175.
- Brems, D., Ganio, M., Latruwe, K., Balcaen, L., Carremans, M., Gimeno, D., Silvestri, A., Vanhaecke, F., Muchez, P., Degryse, P., 2013. Isotopes on the Beach, Part 1: Strontium Isotope Ratios as a Provenance Indicator for Lime Raw Materials used in Roman Glass-making. *Archaeometry* 55, 214–234.
- Brems, D., Degryse, P., 2014a. Trace Element Analysis in Provenancing Roman Glass-making. *Archaeometry* 56, 116–136.
- Brems, D., Degryse, P., 2014b. Trace elements in sand raw materials. In: Degryse, P. (Ed.), Glass Making in the Greco-Roman World: Results of the ARCHGLASS Project. Leuven University Press, Leuven, pp. 69–86.
- Brems, D., Freestone, I., Gorin-Rosen, Y., Scott, R., Devulder, V., Vanhaecke, F., Degryse, P., 2018. Characterisation of byzantine and early Islamic primary tank furnace glass. *J. Archaeol. Sci. Rep.* 23, 722–735.
- Brill, R.H., 1992. Chemical analyses of some glasses from Frattesina. *Journal of Glass Studies* 34, 11–22.
- Brill, R.H., 1994. Laboratory studies of some glasses from Vergina. *Journal of Glass Studies* 36, 11–23.
- Brill, R.H., 1999. Chemical Analyses of Early Glass. 2 vols. Volume 1: Catalogue of Samples. The Corning Museum of Glass, New York.
- Brugmann, B., 2004. Glass beads from early Anglo-Saxon graves: a study of the provenance and chronology of glass beads from early Anglo-Saxon graves, based on visual examination. Oxbow, Oxford.
- Ceglia, A., Cosyns, P., Schibille, N., Meulebroeck, W., 2019. Unravelling provenance and recycling of late antique glass from Cyprus with trace elements. *Archaeol. Anthropol. Sci.* 11, 279–291.
- Cestnik, V., 2009. Željeznodobna nekropola Kaštel kod Buja. Analiza pokopa željeznodobne Istre. Monografije i katalogi 18. Arheološki muzej Istra, Pula.
- Conte, S., Arletti, R., Mermati, F., Gratuze, B., 2016. Unravelling the Iron Age glass trade in southern Italy: the first trace element analyses. *Eur. J. Mineral.* 28, 409–433.
- Conte, S., Arletti, R., Henderson, J., Degryse, P., Blomme, A., 2018. Different glassmaking technologies in the production of Iron Age black glass from Italy and Slovakia. *Archaeol. Anthropol. Sci.* 10, 503–521.
- Conte, S., Matarese, I., Vezzalini, G., Pacciarelli, M., Scarano, T., Vanzetti, A., Gratuze, B., Arletti, R., 2019. How much is known about glassy materials in Bronze and Iron Age Italy? New data and general overview. *Archaeol. Anthropol. Sci.* 11, 1813–1841.
- Cosyns, P., Warremboen, E., Bourgeois, J., Degryse, P., 2005. Pre-Roman glass beads in Belgium. *AIHV, Annales du 16e Congrès London*, 2003, pp. 323–326.
- Ćuković, Z., 2017. Claiming the sea: Bronze Age fortified sites of the north-eastern Adriatic Sea (Cres and Lošinj islands, Croatia). *World Archaeol.* 49, 526–546.
- Davis, M., Freestone, I.C., 2018. Trading North: Glass-working beyond the edge of the empire. In: Rosenow, D., Phelps, M., Meek, A., Freestone, I.C. (Eds.), Things That Travelled: Mediterranean Glass in the First Millennium AD. UCL Press, London, pp. 107–133.
- Degryse, P., Shortland, A., 2009. Trace elements in provenancing raw materials for Roman glass production. *Geol. Belg.* 12, 135–143.
- Eremi, K., Degryse, P., Erb-Satullo, N., Ganio, M., Greene, J., Shortland, A., Walton, M., Stager, L., 2012. Iron Age glass beads from Carthage. In: Meeks, N., Cartwright, C., Meek, A., Mongiatto, A. (Eds.), Historical Technology, Materials and Conservation. SEM and Microanalysis. Archetype Publications in association with the British Museum, London.
- Foy, D., Picon, M., Vichy, M., Thirion-Merle, V., 2003. Caractérisation des verres de la fin de l'Antiquité en Méditerranée occidentale: L'émergence de nouveaux courants commerciaux. In: Foy, D., Nenna, M.D. (Eds.), Échanges et Commerce Du Verre Dans Le Monde Antique: Actes Du Colloque International De L'association Française Pour L'archéologie Du Verre. Montagnac, Éditions Monique Mergoil, pp. 41–85.
- Franjić, A., Freestone, I.C., Krži, B., Stipanić, P., 2022. The spectrometric analysis of Iron Age glass beads from Novo Mesto, Slovenia. *Studia Universitatis Hereditati* 10, 23–29.
- Freestone, I.C., Leslie, K.A., Thirlwall, M., Gorin-Rosen, Y., 2003. Strontium Isotopes in the Investigation of Early Glass Production: byzantine and Early Islamic Glass from the Near East. *Archaeometry* 45, 19–32.
- Freestone, I.C., Stapleton, C.P., 2015. Composition, Technology and production of coloured glasses from Roman mosaic vessels. In: Bayley, J., Freestone, I.C., Jackson, C. (Eds.), Glass of the Roman World. Oxbow Books, Oxford, pp. 61–76.
- Freestone, I.C., Degryse, P., Lankton, J., Gratuze, B., Schneider, J., 2018. HIMT, glass composition and commodity branding in the primary glass industry. In: Rosenow, D., Phelps, M., Meek, A., Freestone, I.C. (Eds.), Things That Travelled: Mediterranean Glass in the First Millennium AD. UCL Press, London, pp. 159–190.
- Freestone, I.C., Barfod, G.H., Chen, C., Larson, K.A., Gorin-Rosen, Y., 2023. Glass production at Jalame, Israel: Process, composition and relationship to Roman glass in Europe. *J. Archaeol. Sci. Rep.* 51, 104179.
- Freestone, I.C., Gorin-Rosen, Y., Hughes, M.J., 2000. Primary glass from Israel and the production of glass in Late Antiquity and the Early Islamic period. In: Nenna, M.D. (Ed.), La Route du Verre. TMO 33, Maison de l'Orient Méditerranéen, Lyon, 2000, pp. 65–84.
- Freestone, I.C., Brems, D., Degryse, P., 2025. Composition of Late Hellenistic to Early Roman glass vessels from the Souk Excavations, Beirut. *Rendiconti Lincei. Scienze Fisiche e Naturali*, February 19, 2025.
- Gabrovec, S., Mihovilić, K., 1987. Istarska grupa In: Benac, A. (Ed.), Prahistorija jugoslavenskih zemalja. 5 vols. Akademija nauka i umjetnosti Bosne i Hercegovine: V. Sarajevo, pp. 293–338.
- Gavranović, M., 2016. In: Gedigi, B., Grossman, A., Piotrowskiego, W. (Eds.), Europa W okresie od VII wieku przed narodzeniem Chrystusa do I wieku naszej ery. Biskupin Wrocław: Archäologisches Museum in Biskupin: Biskupiner Archäologische Arbeiten 11, 21 (Nr.). Polnischen Akademie der Wissenschaften Abteilung Wrocław: Arbeiten Der Archäologischen Kommission, pp. 123–146.
- Giliozzo, E., 2017. The composition of colourless glass: a review. *Archaeol. Anthropol. Sci.* 9, 455–483.
- Gratuze, B., Picon, M., 2005. Utilisation par l'industrie verrière des sels d'aluns des oasis égyptiennes au début du premier millénaire avant notre ère. In: Borgard, P., Brun, J.-P., Picon, M. (Eds.), L'alun De Méditerranée: Colloque International, Naples, 4–6 Juin 2003, Lipari, 7–8 Juin 2003. Centre Jean Bérard, Naples, pp. 269–276.
- Gnirs, A., 1925. Istrija praeromana. Beiträge zur geschichte der frühesten und vorrömischen kulturen an den küsten der nördlichen adria. Mit 88 abbildungen im text. In: Mit unterstützung des Ministeriums für schulwesen und. volkskultur. W. Heinisch, Karlsbad.
- Gratuze, B., 2009. Les premiers verres au natron retrouvés en Europe occidentale: composition chimique et chronotypologie. In: Janssens, K., Degryse, P., Cosyns, P., Caen, J., Van't dack, L. (Eds.), Annales du 17^e Congrès de l'Association Internationale pour Histoire du Verre. Annales of the 17th Congress of the International Association for the History of Glass. University Press Antwerp, Antwerp, pp. 8–14.
- Gratuze, B., Pactat, I., Schibille, N., 2018. Changes in the Signature of Cobalt Colorants in late Antique and Early Islamic Glass Production. *Minerals* 8, 1–20.
- Guillong, M., Hametner, K., Reusser, E., Wilson, S.A., Günther, D., 2005. Preliminary Characterisation of New Glass Reference Materials (GSA-1G, GSC-1G, GSD-1G and GSE-1G) by Laser Ablation-Inductively coupled Plasma-Mass Spectrometry using 193 nm, 213 nm and 266 nm Wavelengths. *Geostand. Geoanal. Res.* 29, 315–331.
- Haevernick, T.E., Dobiat, C., 1987. Glasperlen der vorrömischen Eisenzeit II: Ringaugenperlen und verwandte Perlengruppen. In: Marburger Studien zur Vor- und Frühgeschichte, Bd. 9. Dr. Wolfram Hitzer Verlag, Marburg/Lahn.
- Haevernick, T.E., 1978. Urnenfelderzeitliche Glasperlen, Zeitschrift für schweizerische Archäologie Und Kunstgeschichte 35, 145–157.
- Hartmann, G., Kappel, I., Grote, K., Arndt, B., 1997. Chemistry and Technology of Prehistoric Glass from Lower Saxony and Hesse. *J. Archaeol. Sci.* 24, 547–559.
- Henderson, J., 1988. Glass production and Bronze Age Europe. *Antiquity* 62, 435–451.
- Henderson, J., 2013. Ancient glass: an Interdisciplinary Exploration. Cambridge University Press, Cambridge.
- Henderson, J., Chenery, S., Omura, S., Matsumura, K., Faber, E., 2018. Hittite and Early Iron Age Glass from Kaman Kâle Höyük and Büklükale, Turkey: evidence for local production and Continuity? *Archaeol. Anthropol. Sci.* 21, 70–84.
- Hoernes, M., 1894. Ausgrabungen auf den Castellier von Villanova am Quieto in Istrien. Mitteilungen Des Archaeologische Gesellschaft 24, 155–184.
- Janković, I., Ahern, J.C.M., Mihelić, S., Premuzić, Z., 2015. Bronze and Iron Age Finds from Romuald's Cave, Istria: 2014 Excavation season. *Coll. Antropol.* 39, 943–946.
- Jochum, K.P., Nohl, U., Herwig, K., Lamml, E., Stoll, B., Hofmann, A.W., 2005. GeoReM: a New Geochemical Database for Reference Materials and Isotopic Standards. *Geostand. Geoanal. Res.* 29, 333–338.
- Kaczmarczyk, A., 1986. In: The Source of Cobalt in Ancient Egyptian Pigments. Smithsonian Institution Press, Washington, pp. 369–376.
- Kamber, B.S., Greig, A., Collerson, K.D., 2005. A new estimate for the composition of weathered young upper continental crust from alluvial sediments, Queensland, Australia. *Geochim. Cosmochim. Acta* 69, 1041–1058.
- Komšo, D., 2012. Predgovor = Foreword. In: Urem, D. (Ed.), Limska Gradina: Keramika s područja nekropole [the Limska Gradina hillfort: pottery from the cemetery area]. Arheološki Muzej Istra, Pula, pp. 7–8.
- Lahil, S., Biron, I., Galoisy, L., Morin, G., 2008. Rediscovering ancient glass technologies through the examination of opacifier crystals. *Appl. Phys. A* 92, 109–116.
- Lahil, S., Biron, I., Galoisy, L., Morin, G., 2009. Technological process to produce antimonate opacified glasses throughout history. *Annales Du 17e Congrès De L'association Internationale Pour L'histoire Du Verre*.
- Lahil, S., Biron, I., Cotte, M., Susini, J., 2010. New insight on the *in situ* crystallization of calcium antimonate opacified glass during the Roman period. *Appl. Phys. A* 100, 683–692.
- Livy, 1996. Ab Urbe Condita. Book 40. Trans. P.G. Walsh. Warminster: Aris & Phillips.
- Lončarić, V., Arruda, A.M., Barrulas, P., Costa, M., 2024. An Archaeometric Analysis of Black-Appearing Iron Age Glass Beads from Vinha das Caliças 4 (Portugal). *Heritage* 7, 1265–1297.
- Lü, Q., Henderson, J., Wang, Y., Wang, B., 2021. Natron glass beads reveal proto-Silk Road between the Mediterranean and China in the 1st millennium BCE. *Sci. Rep.* 11, 3537.
- Majnarić-Pandžić, N., 1998. Brončano i željezno doba. In: Dimitrijević, S., Težak-Gregl, T., Majnarić-Pandžić, N. (Eds.), Prapovijest. Zagreb, Naprijed, pp. 159–358.
- Marchesetti, C., 1884. Di alcune antichità scoperte a Vermo presso Pisino d'Istria. *Archeografo Triestino* 10, 416–425.
- Matijasić, R., 1982–83. Arheološki muzej Istra u Puli 1902–1982, *Histria archaeologica* 13–14 (1994), 1–32.
- Mihovilić, K., 1972. Nekropola Gradine iznad Limskog kanala. *Histria Archaeologica* III (2), 289–312.

- Mihovilić, K., 1979. Gradina Punta Kašteja kod Medulina. *Histria Arhaeologica* 10, 37–56.
- Mihovilić, K., 2007. Brončani stamnoi iz Nezakcija. *Scripta Praehistorica in Honorem Biba Teržan, Situla* 44, 613–621.
- Mihovilic, K., 2013a. Histri u Istri: željezno doba Istre [Gli Istri in Istria: L'età del ferro in Istria = the Histri in Istria: the Iron Age in Istria]. *Arheološki Muzej Istre*, Pula.
- Mihovilic, K., 2013b. Castellieri–Gradine of the Northern Adriatic. In: Fokkens, H., Harding, A. (Eds.), *The Oxford Handbook of the European Bronze Age*. Oxford University Press, Oxford.
- Mihovilić, K., Rajić Šikanjić, P., 2016. Nalaz žarnog groba kod Mariškići (Lupoglavl) [Urn burial find at Mariškići (Lupoglavl)]. *Histria Archaeologica* 47, 57–76.
- Mladin, J., 1969. Halštatska nekropola na Gradini iznad Limskog kanala. *Jadranski Zbornik* 7 (1966–69), 289–315.
- Molina, G., Odin, G.P., Pradell, T., Shortland, A.J., Tite, M.S., 2014. Production technology and replication of lead antimonate yellow glass from New Kingdom Egypt and the Roman Empire. *J. Archaeol. Sci.* 41, 171–184.
- Möncke, D., Papageorgiou, M., Winterstein-Beckmann, A., Zacharias, N., 2014. Roman glasses coloured by dissolved transition metal ions: redox-reactions, optical spectroscopy and ligand field theory. *J. Archaeol. Sci.* 46, 23–36.
- Moretti, M., 1983. Necropoli del castelliere mediano di Pizzughi. *Prestoria del Caput Adriae*, Trieste, pp. 153–158.
- Nikita, C., Henderson, J., 2006. Glass analysis from Mycenae, Thebes and Elateia: Compositional evidence for a Mycenaean glass industry. *Journal of Glass Studies* 48, 71–120.
- Oikonomou, A., Henderson, J., Gnade, M., Chenery, S., Zacharias, N., 2016. An archaeometric study of Hellenistic glass vessels: evidence for multiple sources. *Archaeol. Anthropol. Sci.* 1, 97–110.
- Oikonomou, A., 2018. Hellenistic core formed glass from Epirus, Greece. a technological and provenance study. *J. Archaeol. Sci. Rep.* 22, 513–523.
- Oikonomou, A., Henderson, J., Chenery, S., 2020. Provenance and technology of fourth-second century BC glass from three sites in ancient Thesprotia, Greece. *Archaeol. Anthropol. Sci.* 12, 269–284.
- Orlić, I., 2011. Histarsko razdoblje. In: Starac, A. (Ed.), Pula: Radanje Grada. Pula, Arheološki muzej Istre, pp. 7–12.
- Panighello, S., Ortega, E.F., van Elteren, J.T., Šelih, V.S., 2012. Analysis of polychrome Iron Age glass vessels from Mediterranean I, II and III groups by LA-ICP-MS. *J. Archaeol. Sci.* 39, 2945–2955.
- Paynter, S., Jackson, C., 2019. Clarity and brilliance: antimony in colourless natron glass explored using Roman glass found in Britain. *Archaeol. Anthropol. Sci.* 11, 1533–1551.
- Paynter, S., 2008. Links between glazes and glass in mid-2nd millennium BC Mesopotamia and Egypt. In: Shortland, A.J., Freestone, I.C., Rehren, Th. (Eds.), *From Mine to Microscope: Advances in the Study of Ancient Technology*. Oxbow Books, Oxford, pp. 93–108.
- Petešić, S., 2011. Uoči osnutka rimske kolonije. In: Starac, A. (Ed.), Pula: Radanje Grada. Arheološki muzej Istre, Pula, pp. 13–17.
- Phelps, M., Freestone, I.C., Gorin-Rosen, Y., Gratuze, B., 2016. Natron glass production and supply in the late antique and early medieval Near East: the effect of the Byzantine–Islamic transition. *J. Archaeol. Sci.* 75, 57–71.
- Reade, W.J., Freestone, I.C., Simpson, S.J., 2005. Innovation or continuity? Early first millennium BCE glass in the Near East: the cobalt blue glasses from Assyrian Nimrud. *Annales Du 16e Congrès de l'Association Internationale Pour l'Histoire Du Verre*, London, 2003. Nottingham: AIHV, pp. 23–27.
- Reade, W.J., Privat, K.L., 2016. Chemical characterisation of archaeological glasses from the Hellenistic site of Jebel Khalid, Syria by electron probe microanalysis. *Heritage Science* 4, 1–17.
- Reade, W.J., Freestone, I.C., Bourke, S., 2009. Innovation and continuity in Bronze Age and Iron Age glass from Pella in Jordan. *Annales du 17e Congrès de l'Association Internationale pour l'Histoire du Verre*, Antwerp, 2006. Antwerp: AIHV, pp. 47–54.
- Reade, W.J., 2021. The first Thousand Years of Glass-making in the Ancient Near East: Compositional analyses of late Bronze and Iron Age Glasses. Arcaneopress, Oxford.
- Rehren, Th., Pusch, E.B., 2008. Crushed Rock and Molten Salt? some aspects of the primary glass production at Qantir/Pi-Ramesse. In: Jackson, C.M., Wage, E.C. (Eds.), *Vitreous Materials in the Late Bronze Age Aegean*. Sheffield Studies in Aegean archaeology. Oxbow, Oxford, pp. 14–33.
- Rehren, Th., Marić, F., Schibille, N., Stanford, L., Swan, C., 2010. Glass supply and circulation in early Byzantine southern Jordan. In: Drauschke, J., Keller, D. (Eds.), *Glass in Byzantium – Production, Usage, Analyses*. International Workshop Organised by the Byzantine Archaeology Mainz, 17th–18th of January 2008 Römisches Germanisches Zentralmuseum. Schnell & Steiner, Mainz: Römisch-Germanisches Zentralmuseum; Regensburg, pp. 65–81.
- Rolland, J., 2015. Expérimentation archéologique: fabrication de parures celtes à partir d'un bloc de verre brut daté de la fin du IIIe siècle av. J.-C., provenant de l'épave des Sanguinaires a. *Bulletin de l'Association Française pour l'Archéologie du Verre* 121, 123.
- Rolland, J., 2021. Le verre de l'Europe celtique: Approches archéométriques, technologiques et sociales d'un artisanat du prestige au second âge du Fer. Sidestone Press, Leiden.
- Sakara Sučević, M., 2004. Kaštelir. *Prazgodovinska naselbina pri Novi vasi*. Univerza na Primorskem, Koper.
- Sayre, E.V., 1963. The intentional use of antimony and manganese in ancient glasses. In: Matson, F.R., Rindone, G. (Eds.), *Advances in Glass Technology*, Part 2. Plenum Press, New York, pp. 263–282.
- Sayre, E.V., Smith, R.W., 1961. Compositional categories of ancient glass. *Science* 133, 1824.
- Schibille, N., Sterrett-Krause, A., Freestone, I.C., 2017. Glass groups, glass supply and recycling in late Roman Carthage. *Archaeol. Anthropol. Sci.* 9, 1223–1241.
- Schibille, N., Gratuze, B., Ollivier, E., Blondeau, E., 2019. Chronology of early Islamic glass compositions from Egypt. *J. Archaeol. Sci.* 104, 10–18.
- Schreurs, J.W., Brill, R.H., 1984. Iron and sulfur related colors in ancient glasses. *Archaeometry* 26, 199–209.
- Shortland, A.J., 2012. *Lapis Lazuli from the Kiln: Glass and Glassmaking in the Late Bronze Age*. Leuven University Press, Leuven.
- Shortland, A.J., Eremin, K., 2006. The Analysis of Second Millennium Glass from Egypt and Mesopotamia, Part 1: New WDS analyses. *Archaeometry* 48, 581–603.
- Shortland, A.J., Tite, M.S., Ewart, I., 2006. Ancient Exploitation and use of Cobalt Alums from the Western oases of Egypt. *Archaeometry* 48, 153–168.
- Shortland, A., Rogers, N., Eremin, K., 2007. Trace element discriminants between Egyptian and Mesopotamian late Bronze Age glasses. *J. Archaeol. Sci.* 34, 781–789.
- Shortland, A.J., Schroeder, H., 2009. Analysis of first millennium BC glass vessels and beads from the Pichvnari necropolis, Georgia. *Archaeometry* 51, 947–965.
- Shortland, A.J., Kirk, S., Eremin, K., Degryse, P., Walton, M., 2018. The analysis of late bronze age glass from Nuzi and the question of the origin of glassmaking. *Archaeometry* 60, 764–783.
- Spaer, M., 2001. Ancient glass in the Israel Museum: Beads and other small objects. The Israel Museum, Jerusalem.
- Starac, A., 2006. *Gradska četvrt Sv. Teodora*. Pula. Hrvatski Arheološki Godišnjak 2, 235–238.
- Starac, A., 2007. *Gradska četvrt Sv. Teodora*. Pula. Hrvatski Arheološki Godišnjak 3, 263–265.
- Starac, A., 2008. Nalaz rimskog svetišta u četvrti Sv. Teodora u Puli. Arheološka istraživanja 2008. *Histria Archaeologica* 38–39, 123–168.
- Starac, A., 2011. Pula: Radanje grada. Arheološki muzej Istre, Pula.
- Stipčević, A., 1974. Istarski povijest, život, kultura. Školska knjiga, Zagreb.
- Stoddart, S., 2014. A View from the South (West). Identity in Tyrrhenian Central Italy. In: Popa, C.N., Stoddart, S. (Eds.), *Fingerprinting the Iron Age. Approaches to Identity in the European Iron Age. Integrating South-Eastern Europe into the Debate*. Oxford, Oxbow Books, pp. 266–282.
- Šmit, Ž., Lahnar, B., Turk, P., 2020. Analysis of prehistoric glass from Slovenia. *J. Archaeol. Sci. Rep.* 29, 102114.
- Tal, O., Jackson-Tal, R., Freestone, I.C., 2004. New evidence of the production of raw glass at late拜占庭的阿波利农-阿苏夫，以色列。*J. Glass Stud.* 46, 51–66.
- Thirion-Merle, V., 2005. Les verres de Beyrouth et les verres du Haute Empire dans le monde occidental: étude archéométrique. *J. Glass Stud.* 47, 37–53.
- Tomas, H., 2016. Croatia and the Crossroads of Early Greek Seafarers. In: Davison, D., Gaffney, V., Miracle, P., Sofaer, J. (Eds.) Croatia at the crossroads: a consideration of archaeological and historical connectivity: proceedings of a conference held at Europe House, Smith Square, London, 24–25 June 2013 to mark the accession of Croatia to the European Union. Archaeopress, Oxford, pp. 75–84.
- Towle, A., Henderson, J., Bellintani, P., Gambacurta, G., 2001. Fratessina and Adria: report of scientific analyses of early glass from the Veneto. *Padusa* 37, 7–68.
- Towle, A., Henderson, J., 2004. The glass bead game: Archaeometric evidence for the existence of an Etruscan glass industry. *Etruscan Studies* 10, 47–66.
- Tzankova, N., Mihaylov, P., 2019. Chemical characterization of glass beads from the necropolis of Dren-Delyan (6th–4th century BC), Southwest Bulgaria. *Geologica Balcanica* 48, 31–50.
- Urem, D., 2012. Limska Gradina: Keramika s područja nekropole [the Limska Gradina hillfort: pottery from the cemetery area]. Arheološki Muzej Istre, Pula.
- Vachadze, G., Gratuze, B., 2025. Analysis of early Iron age glass beads (8th to 7th c. BC) from the Tsaischi necropolis (Georgia). *J. Archaeol. Sci. Rep.* 62, 105066.
- Van Ham-Meert, A., Dillies, S., Blomme, A., Cahill, N., Claeys, P., Elsen, J., Eremin, K., Gerdes, A., Steuwe, C., Roeflaers, M., Shortland, A., Degryse, P., 2019. A unique recipe for glass beads at Iron Age Sardis. *J. Archaeol. Sci. Rep.* 108, 104974.
- Venclová, N., Hulínský, V., Henderson, J., Chenery, S., Sulová, L., Hlóžek, J., 2011. Late Bronze Age mixed-alkali glasses from Bohemia. *Archeologicke Rozhledy* 63, 559–585.
- Venclová, N., 1990. Prehistoric glass in Bohemia. *Archeologický ústav ČSAV*, Praha.
- Wedeepholt, K.H., Simon, K., Kronz, A., 2011. The chemical composition including the Rare Earth elements of the three major glass types of Europe and the Orient used in late antiquity and the Middle Ages. *Geochemistry* 71, 289–296.
- Wilkes, J.J., 1922. The Illyrians. Blackwell, Oxford.
- Yatsuk, O., Koch, L., Gorghinian, A., Fiocco, G., Davit, P., Giannossa, L.C., Mangone, A., Francone, S., Serges, A., Re, A., Lo Giudice, A., Ferretti, M., Malagodi, M., Iaia, C., Gulmini, M., 2023a. An archaeometric contribution to the interpretation of blue-green glass beads from Iron Age Central Italy. *Heritage Science* 11, 113.
- Yatsuk, O., Gorghinian, A., Fiocco, G., Davit, P., Francone, S., Serges, A., Koch, L., Re, A., Giudice, A.L., Ferretti, M., Malagodi, M., Iaia, C., Gulmini, M., 2023b. Ring-eye blue beads in iron age central Italy-preliminary discussion of technology and possible trade connections. *J. Archaeol. Sci. Rep.* 47, 103763.
- Yatsuk, O., Koch, L., Giannossa, L.C., Mangone, A., Fiocco, G., Malagodi, M., Gorghinian, A., Ferretti, M., Davit, P., Re, A., Lo Giudice, A., Iaia, C., Gulmini, M., 2024a. It is not crystal clear: "nuances" in the selection of raw materials for Iron Age translucent glass revealed by chemical analyses of beads from central Italy. *Archaeol. Anthropol. Sci.* 16, 129.
- Yatsuk, O., Koch, L., Giannossa, L.C., Mangone, A., Fiocco, G., Malagodi, M., Gorghinian, A., Ferretti, M., Davit, P., Re, A., Lo Giudice, A., Iaia, C., Gulmini, M., 2024b. Back to black: Analysis of the earliest natron glass found in Italy. *J. Archaeol. Sci. Rep.* 57, 104648.
- Zaninović, M., 2007. Zemljopisno-povjesni položaj luka Parentija i Nezakcija. *Histria Archaeologica* 36, 115–136.